

Synthetic and Mechanistic Studies of the Ring Opening and Denitrogenation of Pyridine and Picolines by Ti–C Multiple Bonds[†]

Alison R. Fout, Brad C. Bailey, Dominik M. Buck, Hongjun Fan,[‡] John C. Huffman, Mu-Hyun Baik,* and Daniel J. Mindiola*

Department of Chemistry, Molecular Structure Center, Indiana University, Bloomington, Indiana 47405.

[‡]Present address: State Key Laboratory of Molecular Reaction Dynamics, Dalian Institute of Chemical Physics, Chinese Academy of Sciences, 457 Zhongshan Road, Dalian, People's Republic of China 116023.

Received May 1, 2010

The neopentylidene–neopentyl complex (PNP)Ti=CH^tBu(CH₂^tBu) (**1**; PNP[−] = N[2-P(CHMe₂)₂-4-methylphenyl]₂) extrudes neopentane in neat pyridine or picoline (3- or 4-picoline) under mild conditions (25 °C), to generate the transient titanium alkylidyne intermediate (PNP)Ti≡C^tBu (**A**), which subsequently ring-opens the pyridine by ring-opening metathesis of the aromatic N=C bond across the Ti≡C linkage, generating the metallazaabicycles (PNP)Ti(C(^tBu)C₅H₃RNH) (R = H (**2**), 3-Me (**3**), 4-Me (**4**)). Kinetic studies suggest that the C–N activation process obeys a pseudo-first-order process in titanium, with α-hydrogen abstraction being the rate-determining step (the KIE for **1**/**1-d**₃ conversion to **2** was 3.8(3) at 25 °C). The activation parameters are Δ*H*[‡] = 23(3) kcal/mol and Δ*S*[‡] = −4(3) cal/(mol K). The intermolecular *k*_H/*k*_D ratio is close to unity, 1.07(3) at 25 °C, for the conversion of **1** to **2** in pyridine versus pyridine-*d*₅. Detailed theoretical studies suggest the **1** → **2** transformation proceeds in the following order: (i) formation of **A** in an overall endergonic step by α-hydrogen abstraction, (ii) an exergonic binding of pyridine, and (iii) concerted, exergonic [2 + 2] cycloaddition followed by (iv) exergonic ring-opening metathesis and finally (v) a concerted hydrogen atom migration. Complexes **2**–**4** can denitrogenate, that is, completely remove N of the heterocycle at 65 °C over 72 h, when treated with silyl chlorides such as ClSiR₃ (R = Me, ⁱPr, Ph) to cleanly afford the titanium silylimides (PNP)Ti=NSiR₃(Cl) (R = Me (**8**), ⁱPr (**9**), Ph (**10**)) and the corresponding ^tBu-arene organic byproduct. [Et₃Si][B(C₆F₅)₄] also promotes denitrogenation of **2** to yield ^tBu-benzene, but the metal complex could not be characterized from such a reaction. The conversion **2** → **8** was found to have activation parameters Δ*H*[‡] = 30(6) kcal/mol and Δ*S*[‡] = 10(2) cal/(mol K), therefore yielding Δ*G*[‡] ≈ 27 kcal/mol at 298.15 K. A KIE of 1.6(2) at 85 °C was observed when **2**/**2-d**₅ were denitrogenated to **8** in the presence of ClSiMe₃, with the rate of the reaction being insensitive to both the steric nature and concentration of the trialkylsilyl chloride. Denitrogenation leading to **8**–**10** is proposed to occur via a series of steps including a 1,3-hydrogen migration, an electrocyclic rearrangement, a retrocycloaddition, and a Si–Cl addition. The transformations **1** → **2/3/4** and **2/3/4** → **8** can be made cyclic by a series of steps such as deimination of the imide moiety in **8** with 2 equiv of MoCl₅, followed by reduction and transmetalation with LiCH₂^tBu and then oxidatively induced α-hydrogen abstraction. The reactivity of **1** with other heterocycles such as THF, thiophene, and piperidine is also discussed.

Introduction

Hydrodenitrogenation (HDN) is a key process that removes nitrogen contaminants from petroleum- or coal-based

liquid feedstocks, affording ammonia- and nitrogen-free hydrocarbons.^{1–5} Among the ongoing efforts to improve technology for treating alternative fossil fuel feedstocks,^{6,7} such as heavy oils, tar sands, coal, and oil shale, the key components in need of significant progress include HDN, hydrodesulfurization (HDS), and hydrodeoxygenation (HDO), since these are currently performed simultaneously during the hydrotreating process. Typically, reaction conditions are optimized only for HDS and target low-weight fossil fuel feedstocks.⁸

[†] Part of the Dietmar Seyferth Festschrift.

*To whom correspondence should be addressed. E-mail: mbaik@indiana.edu (M.-H.B.); mindiola@indiana.edu (D.J.M.).

(1) Angelici, R. J. *Polyhedron* **1997**, *16*, 3073.

(2) Fish, R. H.; Thormodsen, A. D.; Moore, R. S.; Perry, D. L.; Heinemann, H. *J. Catal.* **1986**, *102*, 270.

(3) Fish, R. H.; Michaels, J. N.; Moore, R. S.; Heinemann, H. *J. Catal.* **1990**, *123*, 74.

(4) Satterfield, C. N. *Heterogeneous Catalysis in Industrial Practice*, 2nd ed.; Krieger: Malabar, FL, 1991.

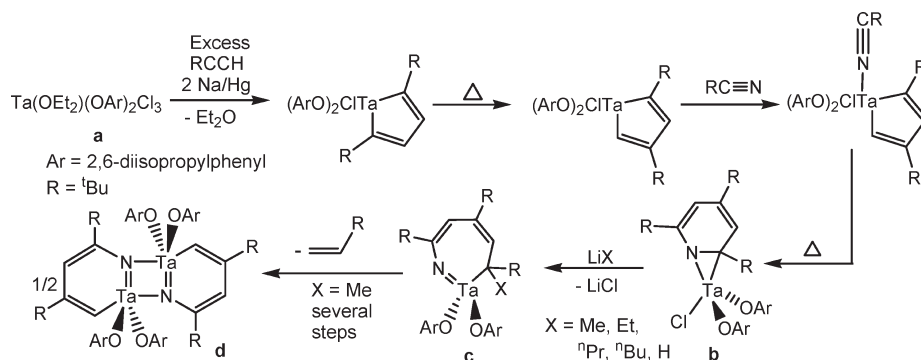
(5) Katzer, J. R.; Sivasubramanian, R. *Catal. Rev. Sci. Eng.* **1979**, *20*, 155.

(6) Leliveld, R. G.; Eijsbouts, S. E. *Catal. Today* **2008**, *130*, 183.

(7) (a) Leckel, D. *Energy Fuels* **2006**, *20*, 1761. (b) Landau, M. V. *Catal. Today* **1997**, *36*, 393. (c) Furimsky, E. *Appl. Catal. A: Gen.* **2000**, *199*, 147. (d) Leckel, D. *Energy Fuels* **2008**, *22*, 231. (e) Rang, H.; Kann, J.; Oja, V. *Oil Shale* **2006**, *23*, 164.

(8) Ho, T. C. *Catal. Rev. Sci. Eng.* **1988**, *30*, 117.

Scheme 1. Preparation of the $\eta^2(N,C)$ -Pyridine Complex **b through a [2 + 2 + 2] Cyclotrimerization, while Salt Metathesis and Alkyl Migration to the α -C Resulted in the C–N Bond Cleavage Product **c** and Finally **d**^a**



^a For simplicity, various intermediates formed during the conversion of **c** to **d** are not shown.³⁴

Consequently, the removal of sulfur and oxygen impurities that constitute the majority of contaminants in crude oil is quite effective,⁹ while nitrogen removal is inefficient under these operating conditions and often captures only the more vulnerable aliphatic amines.^{9–17} N-heterocycles, including pyridine, picolines, quinoline, and heavier analogues, remain untouched and may ultimately poison the catalyst during hydrocracking or serve as the source for hazardous NO_x emissions during combustion of these fuels.^{11,118} The difficulty in N removal arises from the intrinsic strength of the C–N bond, which can be as high as 133 kcal/mol for pyridine.^{19,20} A viable strategy is to dearomatize the N-heterocycles by hydrogenation followed by cleavage of the C–N bond (hydrogenolysis).^{2,3,8,11,22–28} This process comes at a cost, since a requirement for the hydrogenolysis of the C–N bond is the expenditure of H₂ to ultimately form saturated hydrocarbons and ammonia. Recent studies demonstrated that metal surfaces that are chemically treated to carry nitride, carbide, and phosphide groups can efficiently accomplish HDN to give ammonia and hydrocarbons,^{27,29} while being advantageously tolerant of sulfur

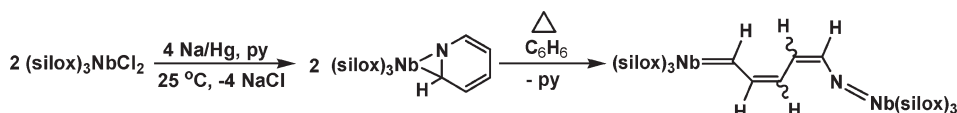
containing impurities found in oil feedstocks.³⁰ Early-transition-metal carbides and nitrides are particularly efficient in this regard. With typical reaction conditions of HDN involving up to 2000 psi of H₂ pressure, 300–500 °C reactor temperature, and the use of poorly defined heterogeneous catalyst formulations based on NiMo/Al₂O₃ or CoMo/Al₂O₃ systems, it is difficult if not impossible to investigate the catalytic mechanism in detail, in particular since intermediates cannot be detected or isolated.^{22–26} Homogeneous models for such catalysts offer an attractive avenue for studying key steps of analogous transformations in which C–N bonds of these N-heterocycles are cleaved under much milder and better defined conditions. These studies may provide important clues for understanding the role of the catalyst and ultimately improving the ineffective standard process of N removal currently in use, which is particularly desirable for middle or heavy distillates derived from shale or tar sands that are known to contain significantly higher amounts of N-heterocycles.²⁷

To date, only two homogeneous metal systems^{31,32} have been reported to mediate C–N bond cleavage of aromatic N-heterocycles relevant to HDN,^{24–26,33–36} while homogeneous systems that fully denitrogenate N-heterocycles are unknown.³² The seminal works by Wigley^{24,33,34,37} and Wolczanski^{35,36,38} provide the only examples of well-defined homogeneous HDN models capable of promoting the C–N bond cleavage of pyridine.²⁸ Common to both systems is the formation of an $\eta^2(N,C)$ -bound pyridine complex with a highly reducing group 5 metal center, while the C–N bond cleavage step entails divergent pathways such as alkyl migration^{33,34} and reduction^{35,36} in the Wigley and Wolczanski

- (9) Laine, R. M. *Catal. Rev. Sci. Eng.* **1983**, *25*, 459.
 (10) Sivasubramanian, R.; Crynes, B. L. *Ind. Eng. Chem. Process Des. Dev.* **1979**, *18*, 175.
 (11) Laine, R. M. *Ann. N.Y. Acad. Sci.* **1983**, *415*, 271.
 (12) Laine, R. M. *New J. Chem.* **1987**, *11*, 543.
 (13) Kabir, S. E.; Day, M.; Irving, M.; McPhillips, T.; Minassian, H.; Rosenberg, E.; Hardcastle, K. I. *Organometallics* **1991**, *10*, 3997.
 (14) Shvo, Y.; Laine, R. M. *J. Chem. Soc., Chem. Commun.* **1980**, 753.
 (15) Adams, R. D.; Chen, G. *Organometallics* **1992**, *11*, 3510.
 (16) Adams, R. D.; Chen, G. *Organometallics* **1993**, *12*, 2070.
 (17) Adams, R. D.; Chen, L.; Wu, W. *Organometallics* **1993**, *12*, 4962.
 (18) Laine, R. M. *J. Mol. Catal.* **1983**, *21*, 119.
 (19) Schmidt, M. W.; Truong, P. N.; Gordon, M. S. *J. Am. Chem. Soc.* **1987**, *109*, 5217.
 (20) Priyajumar, U. D.; Dinadayalane, T. C.; Sastry, G. N. *Chem. Phys. Lett.* **2001**, *337*, 361.
 (21) Fish, R. H. *Ann. N.Y. Acad. Sci.* **1983**, *415*, 292.
 (22) Laine, R. M. *New J. Chem.* **1987**, *11*, 543.
 (23) Sanchez-Delgado, R. A. *Organometallic Modeling of the Hydrodesulfurization and Hydrodenitrogenation Reactions*; Kluwer: Dordrecht, The Netherlands, 2002.
 (24) Weller, K. J.; Fox, P. A.; Gray, S. D.; Wigley, D. E. *Polyhedron* **1997**, *16*, 3139.
 (25) Angelici, R. J. *Polyhedron* **1997**, *16*, 3073.
 (26) Bianchini, C.; Meli, A.; Vizza, F. *Eur. J. Inorg. Chem.* **2001**, 43.
 (27) Furimsky, E.; Massoth, F. E. *Catal. Rev.* **2005**, *47*, 297.
 (28) Regioselective reductive cleavage of a C=C bond in quinoxaline has been reported: Sattler, A.; Parkin, G. *Nature* **2010**, *463*, 523.
 (29) (a) Qian, K.; Rodgers, R. P.; Hendricksen, C. L.; Emmett, M. R.; Marshall, A. G. *Energy Fuels* **2001**, *15*, 492. (b) Bunger, J. W.; Russell, C. P.; Cogswell, D. E. *Am. Chem. Soc. Div. Petr. Chem. Prepr.* **2001**, *46*, 355. (c) Mushrush, G. W.; Beal, E. J.; Hardy, D. R.; Hughes, J. M. *Fuel Proc. Technol.* **1999**, *61*, 197.

- (30) (a) Choi, J.; Brenner, J. R.; Colling, C. W.; Demczyk, B. G.; Dunning, J.; Thompson, L. T. *Catal. Today* **1992**, *15*, 201. (b) Schlatter, J. C.; Oyama, S. T.; Metcalfe, J. E., III; Lambert, J. M., Jr. *Ind. Eng. Chem. Res.* **1988**, *27*, 1648.
 (31) Bailey, B. C.; Fan, H.; Huffman, J. C.; Baik, M.-H.; Mindiola, D. J. *J. Am. Chem. Soc.* **2006**, *128*, 6798.
 (32) Fout, A. R.; Bailey, B. C.; Tomaszewski, J.; Mindiola, D. J. *J. Am. Chem. Soc.* **2007**, *129*, 12640.
 (33) Gray, S. D.; Smith, D. P.; Bruck, M. A.; Wigley, D. E. *J. Am. Chem. Soc.* **1992**, *114*, 5462.
 (34) Gray, S. D.; Weller, K. J.; Bruck, M. A.; Briggs, P. M.; Wigley, D. E. *J. Am. Chem. Soc.* **1995**, *117*, 10678.
 (35) Kleckley, T. S.; Bennett, J. L.; Wolczanski, P. T.; Lobkovsky, E. B. *J. Am. Chem. Soc.* **1997**, *119*, 247.
 (36) Bonanno, J. B.; Veige, A. S.; Wolczanski, P. T.; Lobkovsky, E. B. *Inorg. Chim. Acta* **2003**, *345*, 173.
 (37) Weller, K. J.; Philippov, I.; Briggs, P. M.; Wigley, D. E. *J. Organomet. Chem.* **1997**, *528*, 225.
 (38) Neithamer, D. R.; Parkanyi, L.; Mitchell, J. F.; Wolczanski, P. T. *J. Am. Chem. Soc.* **1988**, *110*, 4421.

Scheme 2. C–N Bond Cleavage of the $\eta^2(N,C)$ -Pyridine Complex (silox)₃Nb(η^2 -pyridine) To Form the Nb=C and Nb=N Dinuclear Species



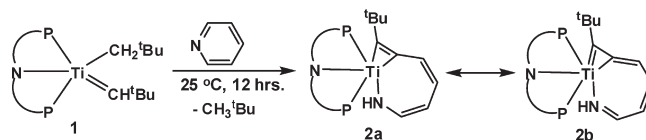
systems, respectively. Wigley's C–N bond cleavage is not the result of the activation of free pyridine from **a**, but rather the result of a preassembled $\eta^2(N,C)$ -pyridine moiety via a set of stepwise reactions (Scheme 1): cycloaddition of two terminal alkynes, followed by isomerization and insertion of a nitrile, to give the pyridine moiety.³⁹ Once the $\eta^2(N,C)$ motif was assembled onto the tantalum metal center to form the "activated" η^2 -pyridine complex **b**, transmetalation of one chloride with either a hydride or alkyl nucleophile, followed by migration of the latter, resulted in the formal cleavage of the C–N bond to afford the ring-opened product **c**.³⁴ A series of elegant and systematic studies revealed that **c** further undergoes several interesting transformations such as β -hydride elimination, reinsertion of the pendant olefin group, an electrocyclic rearrangement, [2 + 2] retrocycloaddition, and finally dimerization to afford the dinuclear metallapyridine species **g**.³⁴ We discuss the work of Wigley, since their work shares transformations similar to those in the work presented herein.

The second example of C–N bond scission of pyridine was reported by Wolczanski using a powerful two-electron reductants.³⁵ The reduction of (silox)₃NbCl₂ (silox[−] = ^tBu₃SiO) with excess amounts of Na/Hg in the presence of pyridine resulted in formation of the $\eta^2(N,C)$ -pyridine adduct (silox)₃Nb(η^2 -pyridine), as highlighted in Scheme 2. Thermolysis of the latter in benzene led to ring opening of pyridine and formed a dinuclear complex containing a Nb=C alkylidene tethered to a Nb=N imido moiety. Consequently, another 1 equiv of free (silox)₃Nb may be critically important to complete the reaction.³⁵

Unfortunately, only a few mechanistic insights were reported for the above-mentioned transformation. Although these reactions were reported over 10 years ago, ring opening of other N-heterocycle analogues by both early- and late-transition-metal complexes has recently seen a renaissance. Diaconescu recently reported the ring opening of 1-methylimidazole by scandium and uranium alkyl complexes.⁴¹ Riera reported the ring opening and subsequent ring contraction of the bipyridine ligand on a tricarbonylrhenium complex using potassium hexamethyldisilazide (KN(SiMe₃)₂) and excess MeOTf as co-reagents.⁴² Recently, Parkin reported an unprecedented C=C reductive cleavage of quinoxaline with a W(II) precursor.²⁸

The urgent need for decreasing the environmental impact of fossil fuel utilization demands a more effective removal of

Scheme 3. Ring-Opening Metathesis of Pyridine To Form Compound 2



sulfur- and nitrogen-containing impurities in fuels,⁴³ which in turn challenges the catalysis research community to better understand the process of C–N rupture and removal, with the ultimate goal of developing improved HDN catalysts. Our goal in this study was to gain a better understanding of the C–N bond breaking event and denitrogenation mechanisms utilizing a well-defined titanium–alkylidene moiety supported by a PNP pincer-type ligand (PNP[−] = N[2-P(CHMe₂)₂-4-methylphenyl]₂). By understanding these important transformations with a simpler system such as ours, we can appreciate the active role of a metal and/or metal–ligand multiple bond in the activation and denitrogenation process. Herein, we describe in detail the ring opening of N-heterocycles and subsequent denitrogenation of pyridine and picolines as well as the reactivity of the transient titanium alkylidene with other heterocycles such as THF, thiophene, and piperidine using various tools of mechanistic inquiry.

Results and Discussion

As mentioned above, previous work on metal surfaces carrying ligands such as nitride, carbide, and phosphide that were effective catalysts for transforming nitrogen contaminants in crude oil to ammonia and hydrocarbons^{27,29} inspired us to question whether or not the reactive intermediate (PNP)Ti≡C^tBu (**A**) can be used as a homogeneous model to probe some of the key steps that are operative in the HDN process. If so, we hoped to obtain an atomistic insight into the mechanism and identify features of the catalytic site that are critical for promoting C–N bond cleavage and, ultimately, N removal. Gratifyingly, our initial attempts of

(43) (a) U.S. Environmental Protection Agency, Air and Radiation, Office of Mobile Sources (EPA420-F-99-051; December 1999). (b) Song, C. *Catal. Today* **2003**, *86*, 211.

(44) Strained metallacyclopropene systems of early metals have revealed highly deshielded α -carbon resonances in the ¹³C NMR spectrum: (a) Buchwald, S. L.; Nielsen, R. B. *Chem. Rev.* **1988**, *88*, 1047. (b) Bennett, M. A.; Wenger, E. *Chem. Ber. Recl.* **1997**, *130*, 1029. (c) Buchwald, S. L.; Watson, B. T.; Huffman, J. C. *J. Am. Chem. Soc.* **1986**, *108*, 7411. (d) Erker, G. *J. Organomet. Chem.* **1977**, *134*, 189. (e) Erker, G.; Kropp, K. *J. Am. Chem. Soc.* **1979**, *101*, 3629. (f) Kropp, K.; Erker, G. *Organometallics* **1982**, *1*, 1246. (g) Buchwald, S. L.; Lum, R. T.; Dewan, J. C. *J. Am. Chem. Soc.* **1986**, *108*, 7441. (h) List, A. K.; Koo, K.; Rheingold, A. L.; Hillhouse, G. L. *Inorg. Chim. Acta* **1998**, *270*, 399. (i) Vaughan, G. A.; Sofield, C. D.; Hillhouse, G. L.; Rheingold, A. L. *J. Am. Chem. Soc.* **1989**, *111*, 5491. (j) McLain, S. J.; Schrock, R. R.; Sharp, P. R.; Churchill, M. R.; Youngs, W. J. *J. Am. Chem. Soc.* **1979**, *101*, 263. (k) Wada, K.; Pamplin, C. B.; Legzdins, P.; Patrick, B. O.; Tsyba, I.; Bau, R. *J. Am. Chem. Soc.* **2003**, *125*, 7035. (l) Wada, K.; Pamplin, C. B.; Legzdins, P. *J. Am. Chem. Soc.* **2002**, *124*, 9680. (m) Threlkel, R. S. Ph.D. Thesis, California Institute of Technology, 1980.

(39) Strickler, J. R.; Bruck, M. A.; Wigley, D. E. *J. Am. Chem. Soc.* **1990**, *112*, 2814.

(40) For an example of a planar metallapyridine system of group 5, see: (a) Weller, K. J.; Filippov, I.; Briggs, P. M.; Wigley, D. E. *Organometallics* **1998**, *17*, 322 and references therein. For a recent paper on metallapyridines, see: (b) Liu, B.; Wang, H.; Xie, H.; Zeng, B.; Chen, J.; Tao, J.; Bin Wen, T.; Cao, Z.; Xia, H. *Angew. Chem., Int. Ed.* **2009**, *48*, 5430.

(41) (a) Carver, C. T.; Diaconescu, P. L. *J. Am. Chem. Soc.* **2008**, *130*, 7558. (b) Monreal, M. J.; Khan, S.; Diaconescu, P. L. *Angew. Chem., Int. Ed.* **2009**, *48*, 8352.

(42) (a) Huertos, M. A.; Perez, J.; Riera, L.; Menendez-Velazquez, A. *J. Am. Chem. Soc.* **2008**, *130*, 13530. (b) Huertos, M. A.; Perez, J.; Riera, L. *J. Am. Chem. Soc.* **2008**, *130*, 5662.

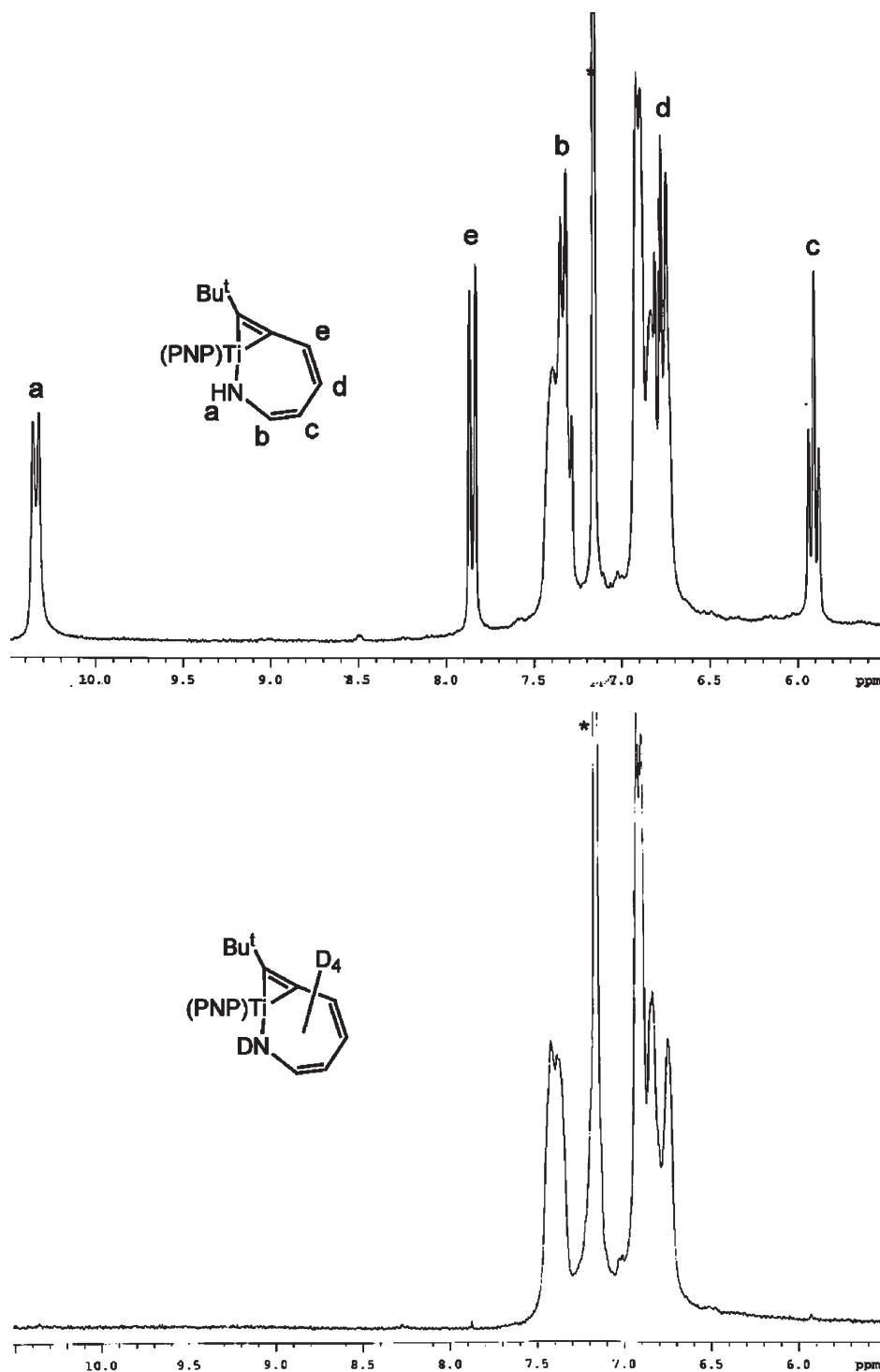


Figure 1. Expanded aryl region of the ^1H NMR spectrum of **2** (top) and **2- d_5** (bottom) with assignments of the azametallabicyclic hydrogens. The asterisk indicates residual protiobenzene in C_6D_6 .

activating pyridine with the Ti–alkylidyne moiety proved successful.

Ring-Opened Products from Pyridine and Picolines. As communicated earlier,³¹ adding pyridine to $(\text{PNP})\text{Ti}=\text{CH}^t\text{Bu}-\text{CH}_2^t\text{Bu}$ (**1**) at room temperature resulted in quantitative formation of the ring-opened product $(\text{PNP})\text{Ti}(\text{C}^t\text{Bu})\text{C}-\text{CC}_4\text{H}_4\text{NH}$ (**2**) (Scheme 3) over 12 h of reaction time. Formation of neopentane is also evident in the ^1H NMR spectrum, but unfortunately, no intermediates were detected by ^{31}P or ^1H NMR spectroscopy over the course of the reaction. Complete

spectroscopic characterization of complex **2** has been discussed previously, and accurate assignment for both the hydrogen and carbon environments was abetted by HMQC and HMBC NMR spectroscopic experiments.³¹

Addition of pyridine- d_5 to **1** afforded $(\text{PNP})\text{Ti}(\text{C}^t\text{Bu})\text{C}-\text{C}_4\text{D}_4\text{ND}$ (**2- d_5**), as we observed and assigned all five hydrogen resonances present in the metallabicyclic motif in **2** by comparison of both the ^1H (Figure 1) and ^2H NMR spectra.³¹ The addition of 98% enriched pyridine- ^{15}N to **1** resulted in the formation of **2- ^{15}N** , $(\text{PNP})\text{Ti}(\text{C}^t\text{Bu})\text{C}_4\text{H}_4^{15}\text{NH}$,

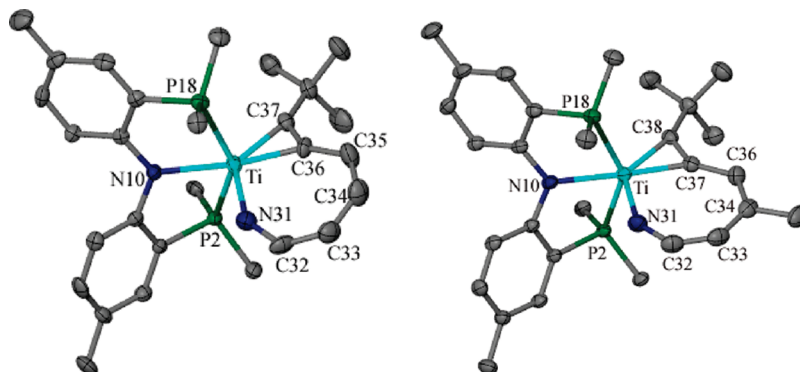


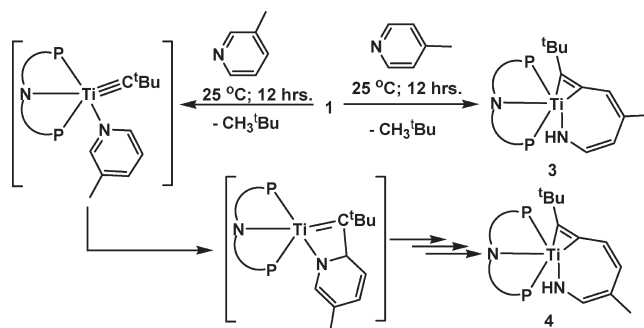
Figure 2. Crystal structures of **2** (left) and **3** (right). Thermal ellipsoids are at the 50% probability level, and ^1Pr methyls and hydrogens have been omitted for clarity. Selected bond lengths (\AA) and angles (deg): for **2**, $\text{Ti1-C36} = 1.986(4)$, $\text{Ti1-C37} = 2.009(3)$, $\text{Ti1-N31} = 1.990(3)$, $\text{Ti1-N10} = 2.195(3)$, $\text{Ti1-P18} = 2.5929(11)$, $\text{Ti1-P2} = 2.6020(11)$, $\text{C36-C37} = 1.313(5)$, $\text{C35-C36} = 1.422(5)$, $\text{C34-C35} = 1.336(6)$, $\text{C33-C34} = 1.406(6)$, $\text{C32-C33} = 1.355(5)$, $\text{N31-C32} = 1.371(5)$, $\text{P18-Ti1-P2} = 146.12(4)$, $\text{Ti1-N31-C32} = 143.9(3)$; for **3**, $\text{Ti1-C38} = 2.010(2)$, $\text{Ti1-C37} = 2.010(2)$, $\text{Ti1-N31} = 1.982(8)$, $\text{Ti1-N10} = 2.193(6)$, $\text{Ti1-P18} = 2.6145(7)$, $\text{Ti1-P2} = 2.6100(7)$, $\text{C38-C37} = 1.330(3)$, $\text{C37-C36} = 1.430(3)$, $\text{C36-C35} = 1.368(3)$, $\text{C34-C33} = 1.427(3)$, $\text{C33-C32} = 1.367(3)$, $\text{N31-C32} = 1.362(3)$, $\text{P18-Ti1-P2} = 145.73(2)$, $\text{Ti1-N31-C32} = 143.1(6)$.

and the ^{15}N NMR spectrum of **2**- ^{15}N displayed a doublet of doublets centered at 131.8 ppm ($^1J_{\text{N-H}} = 58.4$ Hz, $^3J_{\text{N-H}} = 6.0$ Hz). To ascertain the exact connectivity of complex **2**, single-crystal X-ray diffraction studies were conducted to expose a azatitana[7.3]bicyclic framework, shown in Figure 2. The newly formed bond containing C36–C37 has a distance of 1.313(5) \AA and is best described as a metallacyclopropene moiety (also referred to as an η^2 -allenyl moiety) possessing a pendant amide diene, $-\text{CH}=\text{CHCH}=\text{CHNH}$, which is bound to the metal center through the amide nitrogen.³¹ Between the two possible resonance structures **2a,b** shown in Scheme 3, the former structure is most consistent with the X-ray structure.³¹ Alternating bond lengths as suggested by the resonance form **2a** are observed in the crystal structure, as illustrated in Figure 2, and most salient features have been previously discussed.³¹ The short Ti1-N31 bond length of 1.990(3) \AA , compared to the Ti1-N10 bond length of 2.195(3) \AA , indicates a π -bonding interaction of the nitrogen atom with the titanium metal center, while the distances for C32–C33 and C34–C35 are shorter, hence strongly supporting **2a** as the resonance form most consistent with the X-ray crystal structure (Scheme 3).³¹

Addition of 4-picoline to **1** also resulted in the ring-opened product (PNP)Ti(C^tBu)CCHCMeCHNH (**3**), when the mixture was stirred at room temperature for 12 h (Scheme 4). Akin to **2**, complex **3** displayed similar resonances in the ^1H , ^{13}C , and ^{31}P NMR spectra. The solid-state single-crystal structure of **3** also exposed the salient bicyclic ring observed in **2**, with the azatitana[7.3]bicyclic framework fused perpendicularly to the planar PNP ligand (Figure 2). The metric parameters of the solid-state structures of **2** and **3** are virtually identical within experimental error.³¹

Interestingly, ring opening was found to be regioselective for the reaction of **1** with the asymmetric N-heterocycle 3-picoline. Addition of 3-picoline to **1** resulted in the formation of only one product, (PNP)Ti(C^tBu)CCHCMeCHNH (**4**) (Scheme 4),³² which showed ^1H , ^{31}P , and $^{13}\text{C}\{^1\text{H}\}$ NMR spectra that are similar to those of **2** and **3**. Comparison of the ^1H NMR spectrum of **2** with that of **4** allowed us to identify the location of the methyl moiety on the ring. The resonance at 5.61 ppm, which represents the hydrogen on the β -carbon with respect to nitrogen in compound **2**, is no longer present in **4** and the new methyl moiety resonates at 2.29 ppm in the ^1H NMR spectrum. The regioselective

Scheme 4. Ring-Opening Metathesis of 4-Picoline and 3-Picoline To Form **3** and **4**, Respectively



formation of **4** is likely governed by either the binding of pyridine to the transient species **A** or the cycloaddition step, since the bulky *tert*-butyl group of the transient alkylidyne may force the 3-picoline to bind in a facially selective manner with the methyl group pointed away from the metal site (Scheme 4).³² Multiple attempts to isolate the product(s) from **1** and 2-picoline, 2,6-lutidine, and quinoline have failed due to the formation of complicated mixtures. Interestingly, the reaction of **1** with isoquinoline cleanly produces two metal-based products (likely ring-opened products when judged by ^1H NMR spectroscopy), which we are currently trying to separate and fully characterize.

Ring-Opening Mechanism. The experimental observations described above gave a number of important clues. To gain further insight into the conversion of **1** to **2** and derive a complete mechanistic picture, several possible reaction pathways were computationally explored using density functional theory at the B3LYP/cc-pVTZ(-f) level of theory.^{45,46} As shown in Figure 3 and communicated earlier, the initial α -hydrogen abstraction to form **A** is predicted to be the most difficult and thus likely rate-determining, with an activation free energy of 27.5 kcal/mol.³¹ The unsaturated intermediate **A** readily coordinates pyridine to form the pyridine adduct (PNP)Ti \equiv C^tBu(py) (**B**) in an overall exergonic process with a thermodynamic driving force of 10.1 kcal/mol.³¹ The

(45) Becke, A. D. *J. Chem. Phys.* **1993**, 5648. (b) Lee, C. T.; Yang, W.; Parr, R. G. *Phys. Rev. B* **1988**, 37, 785.

(46) *Jaguar 5.5*; Schrödinger, L.L.C., Portland, OR, 1991–2003.

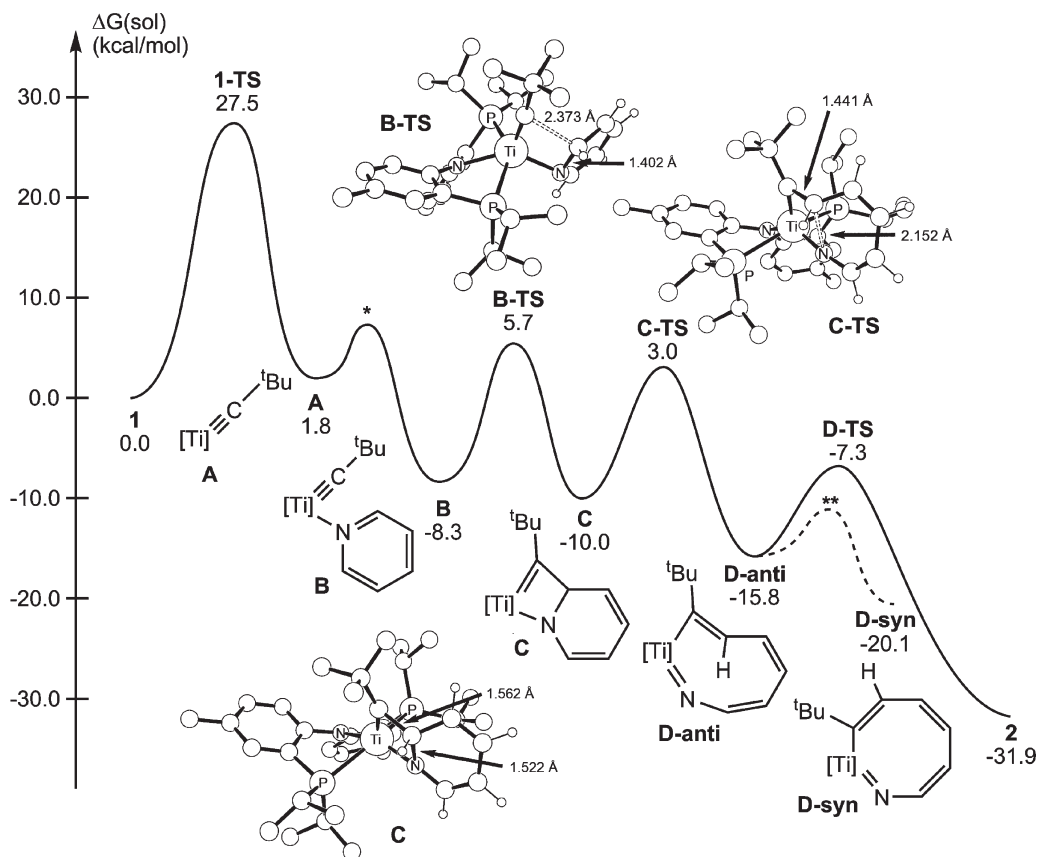


Figure 3. Proposed mechanism for the ring-opening metathesis of pyridine by **1** to form **2**. [Ti] represents the scaffold [(PNP)Ti]. The transition state for initial adduct formation between **1** and pyridine cannot be located on the electronic surface, as it is dominated by the translational entropy change. An estimated barrier of a few kcal/mol is shown for illustrative purposes and marked by a single asterisk. The transition state connecting **D-syn** and **D-anti** was also not located but was estimated by a series of linear transit scans and is marked by two asterisks. **D-TS** is omitted for clarity and is included in the Supporting Information.

Ti≡C^tBu bond length and angle in **A** are virtually unchanged in the structure of **B**, thus suggesting minimal reorganization energy upon binding of the Lewis base. From intermediate **B**, a formal [2 + 2] cycloaddition of the pyridine C–N bond across the highly reactive Ti≡C linkage results in dearomatization of the C–Nπ bond to form **C**. The strained four-membered metallacyclic intermediate **C** was computed to be amenable to ring-opening metathesis (ROM) with a barrier of only 13.0 kcal/mol to afford the ring-expanded titanium imide intermediate **D**, which can exist in two isomeric forms. As depicted in Figure 3, the hydrogen and ^tBu groups may adopt an anti arrangement to each other with the β-hydrogen adjacent to the ^tBu pointing into the ring to afford the stereoisomer **D-anti**. Alternatively, the hydrogen and ^tBu groups may point away from the metal center, adopting an exocyclic orientation and forcing the β-hydrogen and ^tBu moieties to be in a syn orientation, which we labeled as **D-syn** in Figure 3. Due to the strain and slightly puckered nature of the eight-membered ring in the intermediate **D-anti**, its computed energy lies 4.3 kcal/mol higher than that of **D-syn**. Despite significant efforts, we were unable to locate the transition state that connects **D-syn** and **D-anti**, but a systematic exploration of the potential energy surface using various linear transit methods suggests an upper bound of approximately ~4 kcal/mol above the **D-anti** energy for this isomerization reaction, which is readily accessible under normal conditions. The reverse reaction requires an energy of ~8 kcal/mol, which is also easily accessible at room

temperature. Exhaustive explorations of pathways for completing the overall reaction via the **D-syn** intermediate failed thus far and led us to conclude that **D-syn** does not bear a significant mechanistic role. In **D-anti**, the hydrogen is placed perfectly to facilitate the formation of the final product **2**, due to the minimal distance the atom has to travel to reach the product state. Complex **2** is 31.9 kcal/mol lower in energy than **1**,³¹ which is not surprising since the aromatic stability of pyridine has been estimated to be 32 kcal/mol.⁴⁷

As shown in Figure 3, the formation of the reactive titanium alkylidyne intermediate **A** traversing the transition state **1-TS** is the most difficult step overall, with a barrier of 27.5 kcal/mol. The more interesting transition states, however, are **B-TS** and **C-TS** associated with the [2 + 2] cycloaddition and ring-opening metathesis steps, respectively, leading to pyridine ring opening. The coordination geometry of the cycloaddition transition state **B-TS** is best characterized as trigonal bipyramidal, with the main axis being roughly aligned with the P–Ti–P vector. Structurally, this transition state is “early” with the new C–C bond between pyridine and the alkylidyne moiety not being formed to a notable extent at a C–C distance of 2.373 Å and the N–C bond being fully intact at a bond length of 1.402 Å. In the cycloaddition product **C**, the C–C single bond is fully developed at a bond length of 1.562 Å and the bond order of the N–C bond is

(47) Eichler, T.; Hauptmann, S. *The Chemistry of Heterocycles*, 2nd ed.; Wiley-VCH: Weinheim, Germany, 2003.

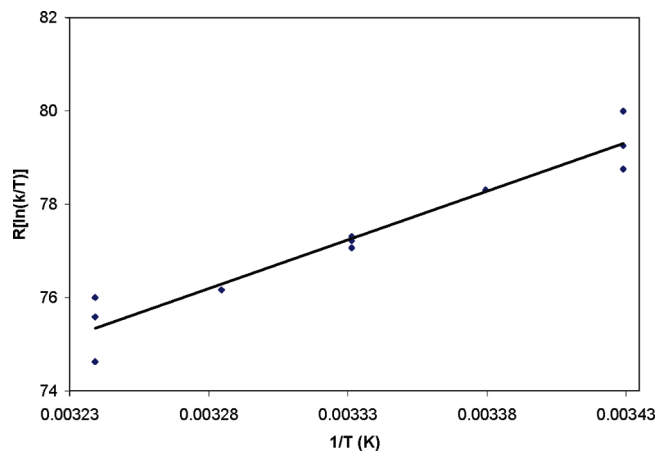
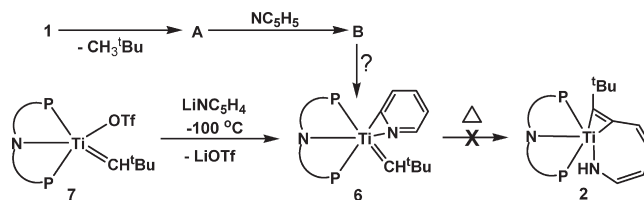


Figure 4. Eyring plot for the conversion **1** → **2** in pyridine.

reduced to **1** with a N–C bond length of 1.522 Å, as illustrated in Figure 3. The σ -bond metathesis transition state **C-TS**, on the other hand, must be considered late, with the N–C bond being essentially broken at a N–C distance of 2.152 Å and the C=C bond having acquired most of the double-bond character at a bond length of 1.441 Å. In the ring-opened product **D-anti** the C=C bond length is 1.374 Å. The transition state **C-TS** leads to the **D-anti** intermediate, because the formal pyridine ring prefers to remain essentially planar, forcing the ^tBu group and the β -hydrogen to adopt an anti orientation to each other. As commented above, the **D-anti** intermediate is higher in energy than **D-syn**, but we believe it to be mechanistically more constructive toward formation of **2**, as indicated in Figure 3.

Although no intermediates were observed by ¹H or ³¹P NMR spectroscopy for the conversion **1** → **2**, which is an expected result since the first step in the reaction is likely rate-determining, as mentioned above, the mechanism outlined in Figure 3 is plausible. We explored the kinetics of the reaction experimentally by ³¹P NMR spectroscopy to confirm that the first step was indeed the slowest and found the reaction to obey a pseudo-first-order rate expression in titanium when pyridine was used as the solvent. Under a depleted amount of pyridine, formation of **2** is not clean, given the ability of intermediate **A** to react with both the solvent and pyridine. Monitoring the reaction from 10 to 35 °C allowed for the extraction of the activation parameters from the Eyring plot, yielding the values $\Delta H^\ddagger = 23(3)$ kcal/mol and $\Delta S^\ddagger = -4(3)$ cal/(mol K), which translates into a ΔG^\ddagger value of ~25 kcal/mol at 298.15 K (Figure 4). The ΔG^\ddagger value is in excellent agreement with the reaction energy profile suggested by our current computer model, as well as the DFT calculations reported for the C–H activation of benzene previously ($\Delta G^\ddagger_{298\text{K}} = 24.7$ kcal/mol).⁴⁸ In fact, the rate for the conversion **1** → **2** ($k_{\text{average}} = 8.4 \times 10^{-5}$ s⁻¹ at 27 °C) is similar to the transformation **1** → (PNP)Ti=CH^tBu(C₆H₅) (**5**) (C–H activation of benzene, $k_{\text{average}} = 6.5 \times 10^{-5}$ s⁻¹ at 27 °C), therefore supporting the notion that these reactions share a similar rate-determining step. A binding event does play an important role in the **1** → **2** transformation, because competition experiments

Scheme 5. Independent Preparation of **6** and Its Thermolysis



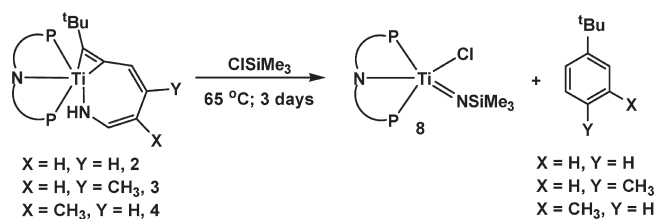
of **1** with pyridine and C₆H₆ (1:1) consistently produced a mixture of **2** and **5** in a ratio of 80:20. The preference for pyridine over benzene is probably due to binding of pyridine to the vacant coordination site of the alkyldyne **A** to afford intermediate **B**. As shown in Figure 3, the energetic driving force for binding pyridine to intermediate **A** is roughly 10 kcal/mol, as opposed to the case for the hypothetical arene adduct **A-C₆H₆**, which is at least 11.3 kcal/mol higher in free energy than **A**.⁴⁸ In accordance with the binding event playing a significant role, a competition reaction of pyridine and pentane (1:1) produced solely the ring-opened pyridine product **2**. When the pyridine to titanium ratio was adjusted to 1:10 in pentane, a mixture of **2** and the C–H activated pentane product(s) was observed, implying that we can only assume zeroth order with respect to the pyridine substrate when such a Lewis base is present in sufficient amounts. Evidence for **A** or **B** being generated in the reaction coordinate leading to **2** was further suggested by an independent reaction. We found that by adding Al(CH₃)₃ to **1**, the alkyldyne can be captured as (PNP)Ti(μ_2 -C^tBu)(μ_2 -CH₃)Al(CH₃)₂, which can react with excess pyridine to form **2** and the adduct (CH₃)₃Al⁻:NC₅H₅.⁴⁹

The intermolecular $k_{\text{H}}/k_{\text{D}}$ ratio was found to be 1.07(3) at 25 °C for the conversion of **1** to **2** in pyridine versus pyridine-*d*₅, therefore establishing that the rate-determining step of the reaction does not involve activation of a pyridine C–H bond. This result is also consistent with the hydrogen shift for **D-anti** to **2** not being rate-determining, which is in accordance with our calculated reaction profile shown in Figure 3. When (PNP)Ti=CD^tBu(CD₂^tBu) (**1-d**₃) was used instead of **1**, however, the KIE for the conversion to **2** in pyridine was found to be 3.8(3) at 25 °C, strongly suggesting that the rate-determining step is α -hydrogen abstraction to form **A**, as anticipated from our computed reaction profile discussed above, as well as previous mechanistic studies for the C–H activation of benzene.⁴⁸

Alternative Pathways to 2. A plausible alternative mechanism by which **B** can convert to **C** is ortho metalation of the α -carbon in free pyridine to form the $\eta^2(N,C)$ -pyridyl species (PNP)Ti=CH^tBu(η^2 -NC₅H₄) (**6**), which has been probed experimentally and theoretically. This mechanism must be considered, since the activation of benzene most likely occurs by a similar mechanism,⁴⁸ and pyridyl complexes of early transition metals have been reported via σ -bond metathesis from the corresponding alkyl precursor and pyridine or picolines.⁵⁰ Experimentally, complex **6** can be synthesized by the reaction of (PNP)Ti=CH^tBu(OTf) (**7**)⁵¹ with LiNC₅H₄⁵² at –100 °C, as shown in Scheme 5.³¹ The pyridyl α -carbon resonance in **6** is in perfect agreement with the analogous complex (PNP)Sc(NHAr)(η^2 -NC₅H₄) (Ar = 2,6-¹Pr₂C₆H₃) reported recently.^{50,53} Although **6** is thermally unstable at room temperature and gives rise to a

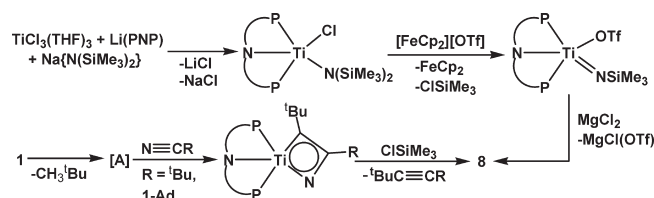
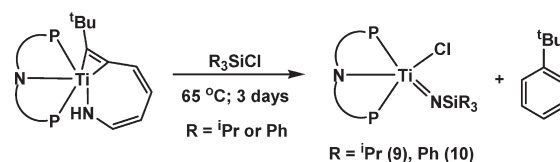
(48) (a) Bailey, B. C.; Fan, H.; Huffman, J. C.; Baik, M.-H.; Mindiola, D. J. *J. Am. Chem. Soc.* **2007**, *129*, 8781. (b) Bailey, B. C.; Fan, H.; Baum, E. W.; Huffman, J. C.; Baik, M.-H.; Mindiola, D. J. *J. Am. Chem. Soc.* **2005**, *127*, 16016. (c) Fout, A. R.; Scott, J. L.; Miller, D. L.; Bailey, B. C.; Huffman, J. C.; Pink, M.; Mindiola, D. J. *Organometallics* **2009**, *28*, 331.

(49) Bailey, B. C.; Fout, A. R.; Fan, H.; Tomaszewski, J.; Huffman, J. C.; Mindiola, J. C. *Angew. Chem., Int. Ed.* **2007**, *46*, 8246.

Scheme 6. Denitrogenation of 2–4 with Chlorotrimethylsilane To Form 8 and the Corresponding Arene

number of products, we were unable to find evidence for the formation of **2** in any amounts detectable by ^1H and ^{31}P NMR spectroscopy. This observation further corroborated the notion that formation of **1** does not progress by C–H activation of pyridine to form **6**.³¹ Computationally, the proposed pathway from **6** to **2** was also investigated, and the unreasonable transition state energies suggest this pathway not to be operative.³¹ Hence, we conclude that the most likely mechanism for the ring opening of pyridine consists of adduct **B** undergoing an unprecedented and concerted [2 + 2] cycloaddition followed by a ring-opening σ -bond metathesis to produce the intermediates **C** and **D-anti**, respectively, as illustrated in Figure 3.

Denitrogenation. Prior to our work, the reports of Wigley³⁴ and Wolczanski³⁵ were two sparse examples (of well-defined species) of pyridine ring opening. However, the shortcoming of both systems is the failure to completely remove the nitrogen from pyridine. In both cases a stable metal–imido species is produced, in part due to the thermodynamically favorable formation of the strong metal–nitrogen multiple bond with the 4d or 5d group 5 metal centers. Although complexes **2–4** are thermally robust to temperatures in the range 120–140 °C, thermolysis of **2** in neat chlorotrimethylsilane (ClSiMe_3) at 65 °C for 3 days resulted in the quantitative transformation to a new metal species, as shown in Scheme 6.³² ^1H and ^{31}P NMR spectroscopic features are

Scheme 7. Independent Syntheses of Complex 8**Scheme 8. Denitrogenation of 2 with Bulky Electrophiles To Form 9, 10, and the Corresponding Arene**

consistent with those of the previously reported titanium trimethylsilylimide ($\text{PNP})\text{Ti}=\text{NSiMe}_3(\text{Cl})$ (**8**) (Scheme 6).⁵⁴ It was assessed that thermolysis of the isotopomer **2- ^{15}N** prepared from **1** and 98% enriched ^{15}N -pyridine in ClSiMe_3 resulted in formation of the ^{15}N -enriched imido complex ($\text{PNP})\text{Ti}=\text{N}^{15}\text{SiMe}_3(\text{Cl})$ (**8- ^{15}N**).³² The ^{15}N NMR spectrum of **8- ^{15}N** displayed a doublet centered at 553.9 ppm ($^2J_{\text{N-P}} = 2.3$ Hz), which unambiguously suggested that the nitrogen of the imido moiety was derived from the denitrogenation of pyridine. Vacuum transfer of the volatiles of a stoichiometric reaction of **2** and ClSiMe_3 in C_6D_6 verified the formation of a single organic product, *tert*-butylbenzene (^1H and ^{13}C NMR spectroscopy). Likewise, addition of ClSiMe_3 to either **3** or **4** under the same conditions as with **2** resulted in denitrogenation and formation of compound **8** as well as the organic products 4-methyl-1-*tert*-butylbenzene and 3-methyl-1-*tert*-butylbenzene, respectively. Characterization of these organic byproducts was verified by ^1H and ^{13}C NMR spectroscopy. Previous work established that complex **8** can be prepared independently by first performing a salt metathesis of $\text{TiCl}_3(\text{THF})_3$, $\text{Li}(\text{PNP})$, and sodium hexamethyldisilazide to form the titanium amide $(\text{PNP})\text{Ti}\{\text{N}(\text{SiMe}_3)_2\}(\text{Cl})$,⁵⁴ followed by a AgOTf -promoted oxidatively induced ClSiMe_3 abstraction and then a salt metathesis using MgCl_2 (Scheme 7).⁵⁴ We have also reported the synthesis of **8** from the addition of ClSiMe_3 to the azametallacyclobutadiene complex $(\text{PNP})\text{Ti}(\text{NC}(\text{tBu})\text{CR})$ ($R = \text{tBu, Ad}$), concurrent with extrusion of the alkyne $\text{RC}\equiv\text{CtBu}$ (Scheme 7).⁵⁵ Complex **8** has also been structurally elucidated by single-crystal X-ray diffraction studies, and thus, its formation and structural identification are unequivocal.⁵⁴

Mechanistic Considerations: Role of the Electrophile. We probed whether ClSiMe_3 was the only electrophile amenable to “promote” denitrogenation of pyridine in compounds **2–4** and whether or not bulkier trialkylchlorosilanes could yield the same result. Reaction of **2** with chlorotriisopropylsilane (ClSi^iPr_3) at 65 °C for 3 days also resulted in denitrogenation of the former N-heterocycle in complex **2** to form the titanium imido chloride $(\text{PNP})\text{Ti}=\text{NSi}^i\text{Pr}_3(\text{Cl})$ (**9**) (Scheme 8). The identity of complex **9** was verified by multinuclear NMR spectroscopy and combustion analysis. The

(50) (a) Diaconescu, P. L. *Curr. Org. Chem.* **2008**, *12*, 1388 and references therein. (b) Jordan, R. F.; Guram, A. S. *Organometallics* **1990**, *9*, 2116. (c) den Haan, K. H.; Wielstra, Y.; Teuben, J. H. *Organometallics* **1987**, *6*, 2053. (d) Soo, H. S.; Diaconescu, P. L.; Cummins, C. C. *Organometallics* **2004**, *23*, 498. (e) Arndt, S.; Elvidge, B. R.; Zeimentz, P. M.; Spaniol, T. P.; Okuda, J. *Organometallics* **2006**, *25*, 793. (f) Elvidge, B. R.; Arndt, S.; Zeimentz, P. M.; Spaniol, T. P.; Okuda, J. *Inorg. Chem.* **2005**, *44*, 6777. (g) Pool, J. A.; Scott, B. L.; Kiplinger, J. L. *J. Alloys Compd.* **2006**, *418*, 178. (h) Jantunen, K. C.; Scott, B. L.; Kiplinger, J. L. *J. Alloys Compd.* **2007**, *444–445*, 363. (i) Thompson, M. E.; Baxter, S. M.; Bulls, A. R.; Burger, B. J.; Nolan, M. C.; Santarsiero, B. D.; Schaefer, W. P.; Bercaw, J. E. *J. Am. Chem. Soc.* **1987**, *109*, 203. (j) Duchateau, R.; van Wee, C. T.; Teuben, J. H. *Organometallics* **1996**, *15*, 2291. (k) Klei, B.; Teuben, J. H. *J. Chem. Soc., Chem. Commun.* **1978**, 659. (l) Klei, E.; Teuben, J. H. *J. Organomet. Chem.* **1981**, *214*, 53. (m) Scollard, J. D.; McConville, D. H.; Vittal, J. J. *Organometallics* **1997**, *16*, 4415. (n) Radu, N. S.; Buchwald, S. L.; Scott, B.; Burns, C. J. *Organometallics* **1996**, *15*, 3913. (o) Watson, P. L. *J. Chem. Soc. Chem. Commun.* **1983**, 276. (p) Dormond, A.; El Bouadili, A. A.; Moise, C. *J. Chem. Soc., Chem. Commun.* **1985**, 914. (q) Boaretto, R.; Roussel, P.; Kingsley, A. J.; Munslow, I. J.; Sanders, C. J.; Alcock, N. W.; Scott, P. *Chem. Commun.* **1999**, 1701. (r) Boaretto, R.; Roussel, P.; Alcock, N. W.; Kingsley, A. J.; Munslow, I. J.; Sanders, C. J.; Scott, P. *J. Organomet. Chem.* **1999**, *591*, 174. (s) Bernskoetter, W. H.; Pool, J. A.; Lobkovsky, E.; Chirik, P. J. *Organometallics* **2006**, *25*, 1092. (t) Bradley, C. A.; Lobkovsky, E.; Chirik, P. J. *J. Am. Chem. Soc.* **2003**, *125*, 8110.

(51) Bailey, B. C.; Huffman, J. C.; Mindiola, D. J.; Weng, W.; Ozerov, O. V. *Organometallics* **2005**, *24*, 1390.

(52) Parham, W. E.; Piccirilli, R. M. *J. Org. Chem.* **1977**, *42*, 257.

(53) Scott, J.; Basuli, F.; Fout, A. R.; Huffman, J. C.; Mindiola, D. J. *Angew. Chem., Int. Ed.* **2008**, *47*, 8502.

(54) Bailey, B. C.; Basuli, F.; Huffman, J. C.; Mindiola, D. J. *Organometallics* **2006**, *25*, 2725.

(55) Bailey, B. C.; Fout, A. R.; Fan, H.; Huffman, J. C.; Brannon Gary, J.; Johnson, M. J. A.; Mindiola, D. J. *J. Am. Chem. Soc.* **2007**, *129*, 2234.

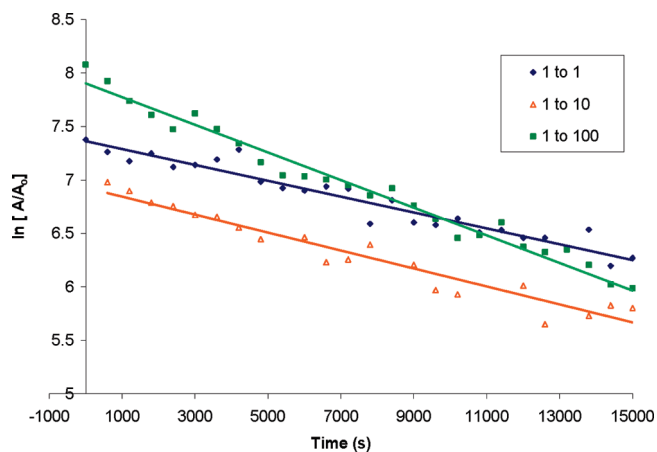


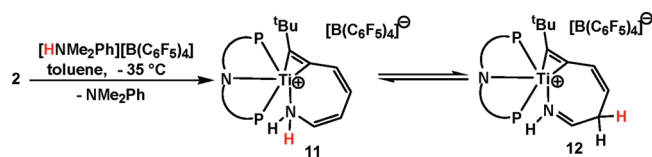
Figure 5. Concentration dependence of ClSiMe_3 on rate in the conversion of **2** to **8** at 80°C .

^{31}P NMR spectrum of **9** displayed two doublets at 27.6 and 18.2 ppm ($^2J_{\text{P-P}} = 54$ Hz). Akin to the isolation of the organic byproducts for the ClSiMe_3 reaction with **2**, the formation of the *tert*-butylbenzene was verified by ^1H and $^{13}\text{C}\{^1\text{H}\}$ NMR spectroscopy. Similarly, addition of chlorotriphenylsilane (ClSiPh_3) to complex **2** at 65°C for 3 days cleanly yielded the red imido complex $(\text{PNP})\text{Ti}=\text{NSiPh}_3(\text{Cl})$ (**10**) (Scheme 8). The synthesis of **10** was also verified by multinuclear NMR spectroscopy, where one of the diagnostic features was the ^{31}P NMR spectrum, displaying two doublets at 29.0 and 21.5 ppm ($^2J_{\text{P-P}} = 65$ Hz). Surprisingly, we found that the rate of the conversion **2** \rightarrow **8** is not dependent on the concentration of ClSiMe_3 at 80°C (0.018 M, $k = [10.2(37)] \times 10^{-5} \text{ s}^{-1}$; 0.18 M, $k = [9.18(23)] \times 10^{-5} \text{ s}^{-1}$; 79.9 M, $k = [11.7(12)] \times 10^{-5} \text{ s}^{-1}$), thus implying that the slow step in the conversion is not the reaction with or activation by the electrophile (Figure 5). The rate of the reaction is also not dependent on the nature of the electrophile, because substituting ClSiMe_3 for ClSi^iPr_3 did not change the rate significantly ($k_{\text{average}} = [1.2(3)] \times 10^{-4} \text{ s}^{-1}$ at 85°C vs $k_{\text{average}} = [1.4(3)] \times 10^{-4} \text{ s}^{-1}$ at 85°C , respectively).

In an effort to further investigate possible intermediates of the denitrogenation process and to ascertain where the electrophile might first add the ring-opened pyridine product, **2** was exposed to a much smaller electrophile, H^+ , derived from $[\text{HNMe}_2\text{Ph}][\text{B}(\text{C}_6\text{F}_5)_4]$.⁵⁶ In this case denitrogenation does not ensue. Instead, the salt product $[(\text{PNP})\text{Ti}(\text{NH}_2\text{C}_5\text{H}_4\text{-}(\text{C}^i\text{Bu}))][\text{B}(\text{C}_6\text{F}_5)_4]$ (**11**) is obtained as a purple-blue oil (Scheme 9). Dimethylaniline was removed by washing the residue with copious amounts of pentane (1 mL, ~ 20 – 30 times) and drying under reduced pressure between each wash, ultimately resulting in an oily blue material. The ^1H NMR spectrum of **11** was clean and revealed one ^iBu group, two sets of multiplets in the aliphatic region (2.75 and 3.34 ppm), two broad singlets in the olefinic region (4.78 and 6.56 ppm), and a resonance corresponding to a N–H group (9.54 ppm). Upon integration, another proton was found to overlap with one of the PNP aryl resonances.

Formation of **11** and its tautomer, $[(\text{PNP})\text{Ti}(\text{NHC}_5\text{H}_4\text{-}(\text{C}^i\text{Bu}))][\text{B}(\text{C}_6\text{F}_5)_4]$ (**12**), were spectroscopically evident when **2-d**₅ was treated with $[\text{HNMe}_2\text{Ph}][\text{B}(\text{C}_6\text{F}_5)_4]$. An overlay of the ^1H NMR spectra for compounds **11** and **12** and the

Scheme 9. Reactivity of **2** with $[\text{HNMe}_2\text{Ph}][\text{B}(\text{C}_6\text{F}_5)_4]$



isotopomers **11-d**₅ and **12-d**₅ is shown in Figure 6. The previously observed diastereotopic hydrogens ($J_{\text{H-H}} = 18$ Hz) in the γ -position, labeled as e in blue in Figure 6, resolved into two singlets (2.73 and 3.34 ppm, red), while incorporation of a proton into the N–D position (9.54 ppm) was clearly evident. No exchange of deuterium into the positions b–d of the ring was evident. Corroborating our findings and proper assignment, the ^2H NMR spectrum of **11-d**₅/**12-d**₅ revealed all six expected deuterium resonances without any deuterium incorporation into the PNP ligand framework. All these observations suggest that a small electrophile such as H^+ binds first to the nitrogen in **2** to form the salt **11** and subsequently tautomerizes to **12**.³² Although it is questionable whether or not a larger electrophile such as $^+\text{SiMe}_3$ undergoes the same chemistry, our kinetic studies clearly suggest that an electrophile larger than H^+ is necessary to achieve denitrogenation.

To better understand the role of the anion in an electrophile such as ClSiR_3 during the denitrogenation sequence, we investigated the reaction of **2** with other electrophiles containing a SiMe_3 group while changing the anion to I, Br, and OTf. Surprisingly, treatment of **2** with XSiMe_3 , where X = I, Br, OTf, or with FSiPh_3 resulted in complicated mixtures. When $[\text{Et}_3\text{Si}][\text{B}(\text{C}_6\text{F}_5)_4]$ ⁵⁷ was added to the ring-opened pyridine product **2**, however, there was an immediate color change from red to purple, resulting in the formation of new products when the mixture was examined by ^{31}P NMR spectroscopy (Scheme 10). Although we were unsuccessful in characterizing the titanium-based products, we were able to verify the formation of the organic byproduct, *tert*-butylbenzene, in this reaction by ^1H NMR spectroscopy of the volatiles.³² After the organic byproduct was separated, attempts to use anion exchange of $[\text{PPN}]\text{Cl}$ or ClCPh_3 with the mixture did not result in the formation of the neutral imide **8**, therefore implying that the cation $[(\text{PNP})\text{Ti}=\text{NSiMe}_3]^+$, if formed, was no longer present in the mixture. Furthermore, independent synthesis of the imido cation from **8** and $\text{Li}(\text{OEt})_2[\text{B}(\text{C}_6\text{F}_5)_4]$ in benzene resulted in no reaction, even after heating at 85°C for 3 days, suggesting that the imido species **8** is relatively stable even under forcing conditions, while the hypothetical species $[(\text{PNP})\text{Ti}=\text{NSiMe}_3]^+$ is not. It is important to note that $[\text{Et}_3\text{Si}][\text{B}(\text{C}_6\text{F}_5)_4]$ did not react with **8** to yield a mixture of intractable materials. In conclusion, we found that the identity of the anion (e.g., Cl^- or $\text{B}(\text{C}_6\text{F}_5)_4^-$) does not impede the denitrogenation reaction.

Role of Solvent and Variance in the N-Heterocycle. When the nitrogen of pyridine is activated, for example as found in adducts such as O^-py , its chemistry deviates significantly from that of the free base, switching from the more common C–H activation mode⁵⁸ to rare transformations such as ring

(57) (a) Lambert, J. B.; Zhang, S.; Ciro, S. M. *Organometallics* **1994**, *13*, 2430. (b) Scott, V. J.; Celenligil-Cetin, R.; Ozerov, O. V. *J. Am. Chem. Soc.* **2005**, *127*, 2852.

(58) Pool, J. A.; Scott, B. L.; Kiplinger, J. L. *J. Am. Chem. Soc.* **2005**, *127*, 1338.

(56) Tjaden, E. B.; Swenson, D. C.; Jordan, R. F.; Peterson, J. L. *Organometallics* **1995**, *14*, 371.

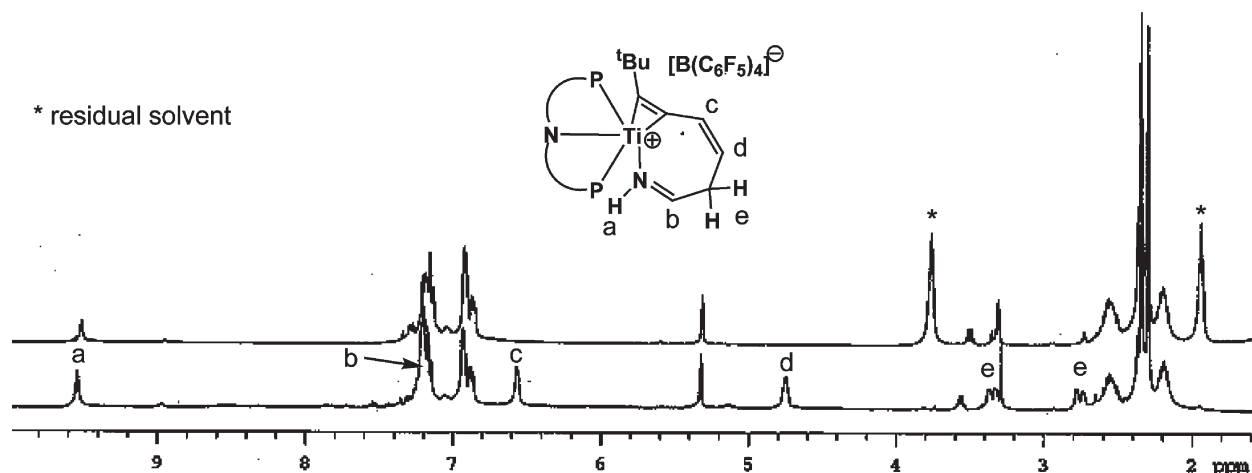
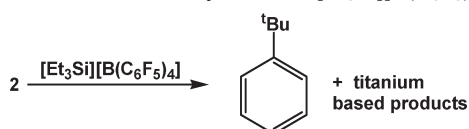
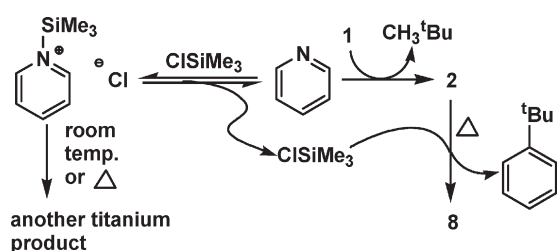


Figure 6. ^1H NMR spectra of the tautomers **12-d₅** (top) and **12** (bottom) showing the incorporation of the proton into the α - and γ -positions of the azametallacycle. The resonance at 5.32 ppm represents residual protio solvent in CD_2Cl_2 . The asterisks denote residual THF solvent.

Scheme 10. Reactivity of **2** with $[\text{Et}_3\text{Si}][\text{B}(\text{C}_6\text{F}_5)_4]$



Scheme 11. Treatment of **1** with py and ClSiMe_3 in Cyclohexane and Subsequent Thermolysis



opening.⁵⁹ For instance, pyridine can be cyclometalated with $\text{Cp}^*\text{Ac}(\text{CH}_3)_2$ ($\text{Ac} = \text{Th}, \text{U}$) to afford pyridyl complexes,⁵⁸ whereas the complex Cp^*ThPh_2 can ring-open 1 or 2 equiv of O^-py to form oximate ligands of the types $\text{Cp}^*\text{Th}(\eta^2\text{-NC}_5\text{H}_4)(\eta^2\text{-ONCHCHCHCHCHPh})$ and $\text{Cp}^*\text{Th}(\eta^2\text{-ONCHCHCHCHCHCHPh})_2$.⁵⁹ In our case, the cyclohexane solution of **1** can be treated with an equal molar amount of pyridine and ClSiMe_3 at room temperature (premixed prior to addition to complex **1**) to form complex **2** along with another titanium product in approximately equal amounts. Thermolysis of the reaction mixture at 65°C over 3 days converts all of **2** to **8** and the corresponding arene byproduct. Surprisingly, thermolysis does not affect the other titanium product originally formed from **1** and the pyridine/ ClSiMe_3 mixture. Although the second titanium product displays olefin-like resonances, on the basis of ^1H NMR spectroscopy and two new ^{13}P NMR spectral resonances, attempts to separate or purify this complex were unsuccessful. Therefore, we propose that the equilibration of $[\text{Me}_3\text{SiNC}_5\text{H}_5][\text{Cl}]$ to ClSiMe_3 and pyridine results in two independent pathways, one of which we know entails the

Eyring Plot for the Formation of 8

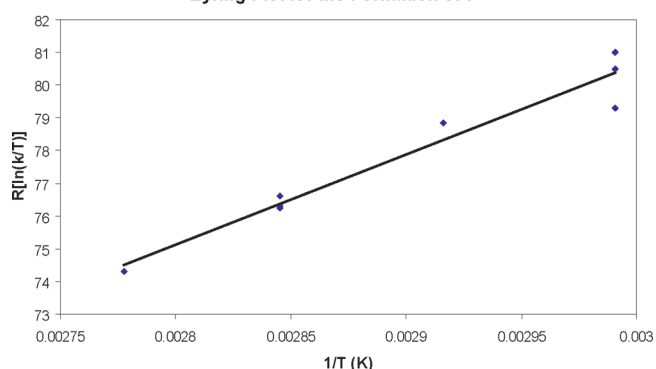


Figure 7. Eyring plot for the conversion of **2** to **8** in C_7D_8 .

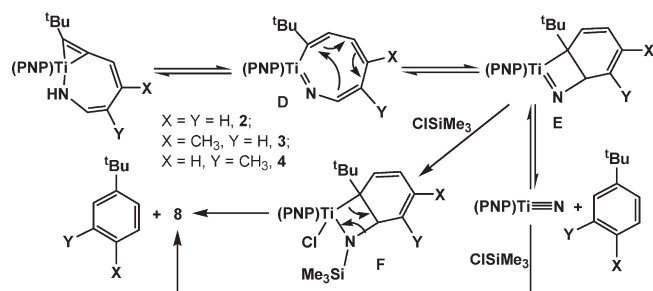
ring opening of pyridine. Further heating of the mixture ensures conversion of complex **2** to **8** via the presence of ClSiMe_3 , while the other titanium product, presumably formed from trimethylsilylpyridinium activation, remains intact (Scheme 11).

Kinetic Isotope Effects and Activation Parameters for the N-Excision Process. The kinetics for the conversion of **2** to **8** was examined by monitoring the decay of **2** at 85°C in toluene using ^{31}P NMR spectroscopy. From our data the reaction was found to obey pseudo-first-order kinetics with respect to titanium ($k_{\text{average}} = [1.2(3)] \times 10^{-4} \text{ s}^{-1}$ at 85°C , vide supra). No intermediates were detected by ^1H or ^{31}P NMR spectra. Temperature-dependence studies of the **2** \rightarrow **8** transformation measured between 65 and 95°C allowed for extraction of the activation parameters from the Eyring plot: $\Delta H^\ddagger = 30(6) \text{ kcal/mol}$ and $\Delta S^\ddagger = 10(2) \text{ cal/(mol K)}$, therefore yielding $\Delta G^\ddagger \approx 27 \text{ kcal/mol}$ at 298.15 K (Figure 7). Not surprisingly, our ΔH^\ddagger and ΔG^\ddagger activation parameters are larger for the denitrogenation step in comparison to the ring-opening step **1** \rightarrow **2**, since the former reaction occurs slowly at 60°C . Unfortunately, we cannot comment on the entropic parameter, since we are presently unsure of which step is the slowest one along the denitrogenation sequence.

Because a C–H bond must be made while a N–H bond must be broken along the sequence **2** \rightarrow **8**, we examined how the rate of the reaction would vary when substituting H for D

(59) Pool, J. A.; Scott, B. L.; Kiplinger, J. L. *Chem. Commun.* **2005**, 2591.

Scheme 12. Proposed Mechanism for the Conversion of 2 to 8



in the metallabicyclic framework of **2**. Our data suggest that the intramolecular $k_{\text{H}}/k_{\text{D}}$ ratio is slightly larger than unity (1.6(2) at 85 °C), when substituting **2** for **2-*d*₅** in the presence of Me_3SiCl (10 equiv) in C_7D_8 , therefore implying the C–H and N–H bond breaking and making to be, or contribute to, the rate-determining step along the **2** → **8** transformation (vide infra). We expect contributions from secondary isotope effects to the measured KIE, given that there must be at least two C–H and one N–H rehybridization events along the **2** → **8** sequence, and we postulate the C–H rehybridization steps to occur after the N–H 1,3-hydrogen shift. Although we cannot identify with certainty which step is rate determining, we have evidence for which steps are not rate determining in the **2** → **8** sequence.

Proposed Reaction Mechanism. Scheme 12 portrays our proposed and revised³² mechanism for the denitrogenation of pyridine and picolines, initiated by a pre-equilibrated set of steps involving precursors **2**–**4** and progressing through plausible intermediates **D**–**F** to ultimately produce the final product **8** and the corresponding arene. The earlier part of the reaction involves a series of pre-equilibrium steps such as a 1,3-shift of the α -hydrogen from the nitrogen atom in the seven-membered metallacycle to the strained metallacyclopentene α -carbon,⁶⁰ which triggers ring expansion to generate the transient intermediate **D**. The formation of **D** represents the microscopic reverse of the last step in the formation of **2** from **1** (vide supra, Figure 3) and should be an uphill reaction by at least 24.6 kcal/mol on the basis of our calculations for the ring opening of pyridine. Our measured $\Delta G^\ddagger = 30$ kcal/mol from activation parameters obtained via the Eyring plot are suggestive of such a step possibly being the slowest in the **2** → **8** transformation. We do not observe any intermediates along this multistep process, since formation of **D** may be the rate-determining step overall. An electrocyclic rearrangement of a boatlike conformation of titanacyclooctatetraene **D** may then form the ring-contracted azatitana[4.6]bicyclic intermediate **E**, where we expect it to traverse a six- π -electrocyclic, disrotatory transition state as predicted by the Woodward–Hoffmann rules.⁶¹ Wigley and co-workers proposed a similar ring contraction step for an eight-membered tantalacycle intermediate, followed by a retro [2 + 2] cycloaddition to release olefin (vide supra, Scheme 2).³⁴ The rehybridization of the sp^3 carbon to sp^2 during the retro [2 + 2] cycloaddition of **F** to **8**, shown in

the bottom part of Scheme 12, may be the source of the observed secondary isotope effect, resulting in the aforementioned intramolecular KIE of 1.6(2). Any change in rehybridization will bring about an isotope effect, and the KIE to rehybridize an sp^3 carbon to sp^2 has been calculated to be 1.43 in the Cope rearrangement,⁶² closely resembling the value obtained in our study. However, the rehybridization of an sp^2 to a sp^3 carbon should give an inverse KIE of around 0.7, allowing us to fairly confidently exclude the conversion of **D** to **E** as the source of the observed KIE. A similar KIE value was obtained for 1,3-hydrogen shifts in cis-oriented groups in late transition metals,⁶³ but larger KIE values are observed for α -hydrogen migration steps in earlier transition metals, where proton migration is reaching a more linear mode of transfer.⁶⁴ We propose that, once intermediate **E** is formed, ClSiMe_3 adds across the more exposed and strained titanium–imide bond, forming Ti–Cl and N–SiMe₃ bonds to afford **F**. We speculate that formation of **E** may precede ClSiMe_3 addition, given that a similar titanium metallacycle, specifically the azametallacyclobutadienes $(\text{PNP})\text{Ti}(\text{NC}(\text{tBu})\text{CR})$ ($\text{R} = \text{tBu}, \text{Ad}$), react rapidly with ClSiMe_3 to yield **8** and the alkyne $\text{tBuC}\equiv\text{CR}$, as shown in Scheme 7. The driving force to release a sterically encumbered arene in **F** should enable a facile final [2 + 2] retrocycloaddition step and render it irreversible to afford **8** and the arene product. Conversion of **E** to a hypothetical nitride intermediate, $(\text{PNP})\text{Ti}\equiv\text{N}$, followed by rapid 1,2-SiMe₃ addition across the $\text{Ti}\equiv\text{N}$ bond, as indicated in Scheme 12, is also a possibility, but we argue against such a pathway for the following two reasons: first, formation of $(\text{PNP})\text{Ti}\equiv\text{N}$ should be a thermodynamically uphill process, since this molecule should be isolobal with the transient key intermediate **A**. Second, azametallacyclobutadienes of the type $(\text{PNP})\text{Ti}(\text{NC}(\text{tBu})\text{CR})$ that closely resemble **E** do not exchange with either $^{15}\text{N}\equiv\text{CR}$ or alkynes in the absence of ClSiMe_3 even under forcing conditions, indicating that four-membered rings of this kind do not equilibrate to $(\text{PNP})\text{Ti}\equiv\text{N}$ and alkyne.⁵⁵ Likewise, any mechanism that may include a direct addition of ClSiMe_3 to **2**–**4** to promote ring expansion is inconsistent with our observation that the rate of the **2** → **8** transformation is insensitive to electrophile concentration (Figure 5). Our kinetic studies corroborate this speculation, since intermediates cannot be detected by either ^1H or ^{31}P NMR spectroscopy. However, alkyne elimination from $(\text{PNP})\text{Ti}(\text{NC}(\text{tBu})\text{CR})$ is not as facile as an extrusion of benzene in a putative intermediate **E** and the mechanism of denitrogenation via titanium nitride formation cannot be completely ruled out. Extensive computational work gave some support for this part of the mechanism but also revealed that there are a number of unresolved details, particularly regarding the nature of the transition states connecting the various intermediates (e.g., one phosphine arm dissociating from the complex). More computational work is currently in progress in our laboratories.

Cyclic Denitrogenation. Although complex **8** is a thermodynamic sink, powerful electrophiles can deiminate the trimethylsilylimide moiety of this molecule readily, concurrent with the formation of the known complex $(\text{PNP})\text{TiCl}_3$ (**13**). Generation of complex **13** has been confirmed by comparison of the ^1H and ^{31}P NMR spectroscopic data to those for independently prepared samples from addition of

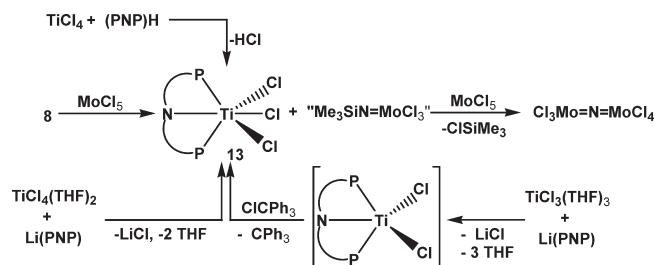
(60) Fleming, I. *Pericyclic Reactions*; Oxford Science Press: Oxford, U.K., 1999.

(61) (a) Woodward, R. B.; Hoffmann, R. *The Conservation of Orbital Symmetry*; Verlag Chemie: Weinheim, Germany, 1970. (b) Vollmer, J. J.; Servis, K. L. *J. Chem. Educ.* **1968**, *45*, 214. (c) Hoffmann, R.; Woodward, R. B. *Acc. Chem. Res.* **1968**, *1*, 17. (d) Haddon, R. C. *Acc. Chem. Res.* **1988**, *21*, 243. It is also possible for these ring-expanded titanium complexes in conjugation to undergo radical based transformations.

(62) Shiner, V. J.; Neumann, T. E. *Z. Naturforsch., A* **1989**, *44*, 337.

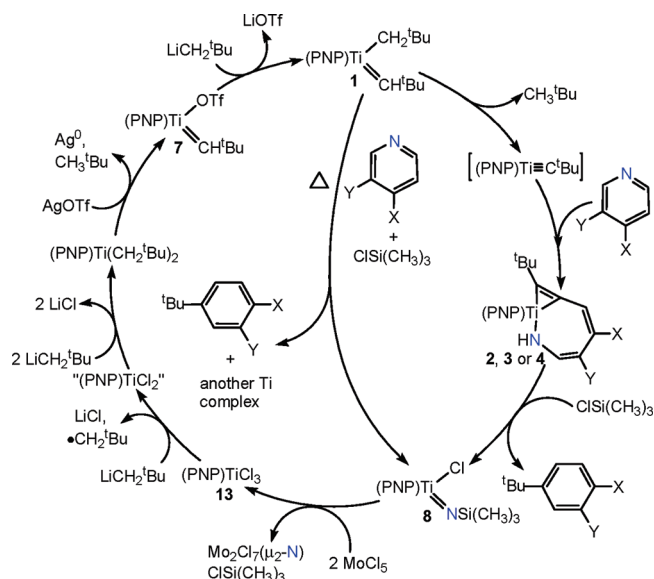
(63) Vicic, D. A.; Jones, W. D. *J. Am. Chem. Soc.* **1999**, *121*, 4070.

(64) Caulton, K. G.; Chisholm, M. H.; Streib, W. E.; Xue, Z. *J. Am. Chem. Soc.* **1991**, *113*, 6082.

Scheme 13. Deimination of 8 with 2 Equiv of MoCl₅ and Independent Routes to Complex 13

(PNP)H to TiCl₄,⁵¹ addition of Li(PNP) to TiCl₄(THF)₂,⁵¹ or by oxidation of “(PNP)TiCl₂” with ClCPh₃ (Scheme 13). The last two reactions give **13** in much cleaner and higher yields than the former. We also inquired whether or not product **8** could be recycled back to **1** by extracting the imide portion and replacing it with two chlorides. We found that **8** could be deiminated with a variety of electrophiles, such as TiCl₄(THF)₂, PCl₅, NbCl₅, and TaCl₅ to afford (PNP)TiCl₃ (**13**) and side product(s).³² However, in these reactions it proved difficult to separate the imide product (or phosphazene product in the case of PCl₅) from **13**, due to their solubility profiles being too similar. Therefore, it was necessary to find a compound that would produce an insoluble byproduct. A review of the literature revealed that the dinuclear nitride complex Mo₂Cl₇(μ₂-N) is insoluble in most organic solvents,⁶⁵ and we hypothesized that such a nitride could stem from the combination of two precursors such as “Me₃SiN=MoCl₃” and MoCl₅ via ClSiMe₃ elimination (Scheme 13). Accordingly, the addition of 2 equiv of MoCl₅ to **8** in benzene resulted in the formation of **13** in 73% yield, concurrent with precipitation of a black insoluble product and formation of ClSiMe₃ (verified by ¹H NMR spectroscopy; Scheme 13). We propose the insoluble byproduct to be Mo₂Cl₇(μ₂-N),⁶⁵ which allows for facile separation of **13** from the reaction mixture.

To close the denitrogenation cycle, complex **13** was converted to the alkylidene precursor “(PNP)TiCl₂” or (PNP)-Ti(CH₂^tBu)₂. Unfortunately, one-electron-reduction reactions of **13** with strong reductants (i.e., Na/Hg, KC₈, and Na(C₁₀H₈)) in various solvents did not afford cleanly the Ti(III) dichloride complex (PNP)TiCl₂.⁵¹ Therefore, we proceeded to reduce **13** in situ and transform it directly to a more stable entity in an effort to avoid ligand disproportionation or other competing over-reduction pathways. Accordingly, addition of 3 equiv of LiCH₂^tBu to **13** cleanly afforded the Ti^{III} species (PNP)Ti(CH₂^tBu)₂ in 75% isolated yield.³² The reaction probably proceeds via an initial reduction of **13** to “(PNP)TiCl₂” by 1 equiv of LiCH₂^tBu as a sacrificial reductant followed by transmetalation of “(PNP)-TiCl₂” with the remaining amount of alkyl reagent to afford (PNP)Ti(CH₂^tBu)₂. Following the known protocol for the synthesis of **1**, oxidatively induced α-hydrogen abstraction of (PNP)Ti(CH₂^tBu)₂ by AgOTf resulted in clean formation of **7** in 85% isolated yield concomitant with precipitation of Ag⁰ and extrusion of CH₃^tBu.⁵¹ Transmetalation of **7** with 1 equiv of LiCH₂^tBu gave **1** in 88% isolated yield, therefore closing the cycle for the denitrogenation of pyridine and picoline by an organometallic titanium reagent (Scheme 14). Since conversions of **1** to **2** and of **2** to **8** are

Scheme 14. Cycle for the Denitrogenation of Pyridine and Picolines

essentially quantitative, the overall yield of the cycle based on titanium reagent (18%) depends on the isolation of **13**, (PNP)Ti(CH₂^tBu)₂, **7**, and **1**. The key to converting the thermodynamically stable complex **8** to a reactive species such as **1** requires the use of a high-energy reagent such as LiCH₂^tBu. Given that the cycle requires a one-electron redox step, the recycling of Ti cannot be made catalytic due to the incompatibility of reagents (e.g., AgOTf, LiCH₂^tBu, MoCl₅, and possibly ClSiMe₃). Scheme 14 also illustrates how formation of **8** from **1** can be achieved (albeit not cleanly, vide supra) directly by adding a premixed solution of pyridine/ClSiMe₃ to **1**.

Reactivity of 1 with Other Heterocycles. Given the remarkable ability of the transient titanium alkylidyne intermediate to ring-open pyridine and picoline, other heterocycles were explored to determine the generality of this process. It is known that the early-transition-metal complex Cp₂ZrSiMe₃(Cl) can ring-open 2-thienyl and 2-furyl under thermal conditions by a migration,^{50,66} while the low-valent species (silox)₃Ta or η⁹:η⁵-bis(indenyl)zirconium sandwich complexes can reductively ring-open THF and its close relatives.⁶⁷ Complex **1** was treated with neat THF with the idea to promote ring opening of the cyclic ether, and the reaction was monitored by ³¹P NMR spectroscopy, resulting in decay of the AB doublets of **1** to a set of singlets at 24.0 and 0.38 ppm. The estimated *t*_{1/2} to formation of the new product was virtually identical with that observed for the ring opening of pyridine, thus suggesting both reactions to have similar rate-determining steps. The fact that no *J*_{P-Ti} was observed suggested tantalizingly that each phosphorus arm of the PNP ancillary was experiencing a significantly different environment without a transoid orientation. A series of six multiplets, not derived from the PNP ancillary ligand, are observed in the ¹H NMR spectrum in the range

(66) Erker, G.; Petrenz, R.; Krueger, C.; Lutz, F.; Weiss, A.; Werner, S. *Organometallics* **1992**, *11*, 1646.

(67) (a) Bonanno, J. B.; Henry, T. P.; Neithamer, D. R.; Wolczanski, P. T.; Lobkovsky, E. B. *J. Am. Chem. Soc.* **1996**, *118*, 5132. (b) Bradley, C. A.; Veiros, L. F.; Pun, D.; Lobkovsky, E.; Keresztes, I.; Chirik, P. J. *J. Am. Chem. Soc.* **2006**, *128*, 16600. (c) Bradley, C. A.; Veiros, L. F.; Chirik, P. J. *Organometallics* **2007**, *26*, 3191.

(65) Godemeyer, T.; Dehnicke, K. *Z. Anorg. Allg. Chem.* **1988**, *558*, 114.

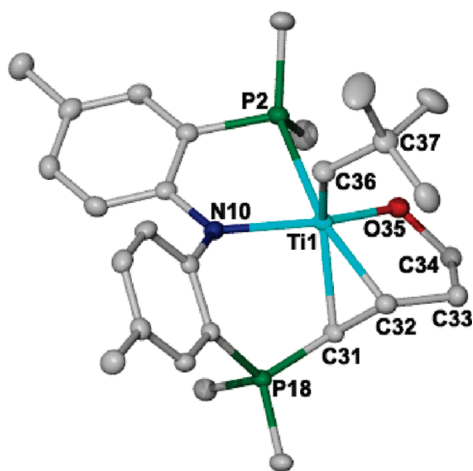
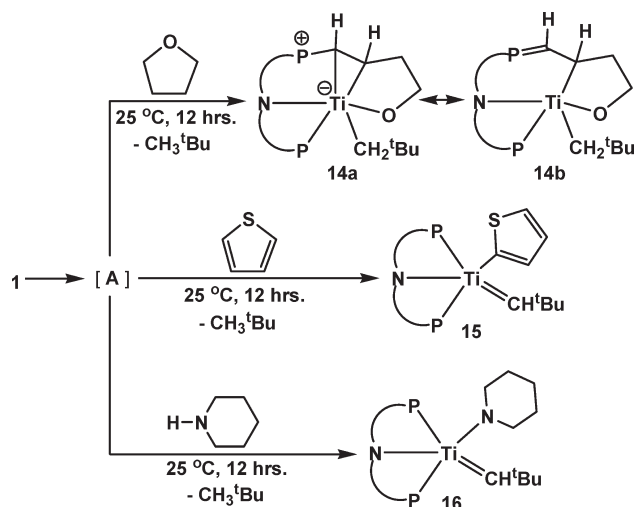


Figure 8. Solid-state diagram of complex **14** displaying thermal ellipsoids at the 50% probability level. All H atoms and isopropyl methyls on phosphorus have been omitted for the purpose of clarity. Selected bond lengths (Å) and angles (deg): Ti1–O35, 1.8874(13); Ti1–N10, 2.1228(15); Ti1–C32, 2.1384(18); Ti1–C36, 2.157(2); Ti1–C31, 2.1920(18); Ti1–P2, 2.7039(6); P18–C31, 1.7277(19); O35–C34, 1.415(2); C31–C32, 1.473(3); C32–C33, 1.518(3); C33–C34, 1.532(3); C37–C36–Ti1, 129.10(14); O35–Ti1–N10, 141.51(6); C32–Ti1–C36, 92.56(8); C32–Ti1–C31, 39.76(7); C36–Ti1–C31, 122.17(8); C32–Ti1–P2, 160.31(5); C31–Ti1–P2, 137.76(6); C36–Ti1–P2, 98.51(6); C34–O35–Ti1, 120.29(11); C31–C32–Ti1, 72.08(10); C33–C32–Ti1, 108.94(12).

1.74–5.04 ppm, all of which are in accord with six different hydrogen environments and the presence of one neopentyl ligand. When the reaction was performed in THF-*d*₈, all six resonances were absent, suggesting that all six of the signals are derived from the cyclic ether. Treating THF-*d*₈ with **1** incorporated deuterium in the methylene moiety of the neopentyl group, concurrent with formation of only CH₃¹Bu, thus suggesting that elimination of the alkane preceded the C–H/C–O bond activation steps. Due to the asymmetry of the product, a combination of ¹³C, ¹³C{¹H}, DEPT, DQCOSY, and HMQC spectroscopic experiments was necessary to partially resolve the connectivity of the THF ring-opened product, in which one of the phosphorus arms of the PNP was significantly transformed. The complex nature for both the ¹H and ¹³C NMR spectra of this new product also provided the impetus to unambiguously confirm its connectivity with a single-crystal X-ray diffraction study. Figure 8 depicts the structure of the product deriving from C–H activation and ring opening of the C–O bond in THF, (PNP)CHCHCH₂CH₂O)Ti(CH₂¹Bu) (**14**). Although the neopentyl group suffers from occupational disorder, all the hydrogen atoms with the exception of the disordered ¹Bu group were located in subsequent Fourier maps and included as isotropic contributors in the final cycles of refinement. The solid-state structure of **14** has many unique features, the most important of which entails the fusing of an oxometallacyclopentane, a metallacyclopropane, and a six-atom azaphosphonium metallacycle. Hence, the three fused rings give a low-symmetry complex with an overall puckered structure. Due to quaternization of a phosphorus atom, only a phosphine moiety of the former PNP ligand now coordinates to Ti. In the solid-state structure, both the Ti1–C36 distance and Ti1–C36–C37 angle are consistent with a neopentyl alkyl ligand, and ring opening of THF results in C–C

Scheme 15. Reaction of **1** with Other Heterocycles To Form Complexes **14**–**16**



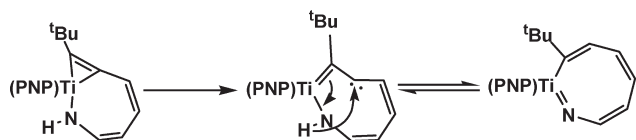
distances all in the range of single bonds, with C31–C32 being the shortest distance (1.473(3) Å). Perhaps the most intriguing feature of **14** is the P18–C31 distance of 1.7277(19) Å, which is in accord with the short distance observed for the ylide motif of Me₂C=P¹Pr₃ (1.731 Å).⁶⁸ Complex **14** can be best described in two canonical forms arising from the ylide character of one phosphine pendant arm composing the former PNP ligand (Scheme 15). Although significantly more work remains to be completed before we can be more certain about the mechanism of the reaction leading to **14**, our isotopic labeling study for this reaction suggests this pathway to proceed via formation of **A**, followed by a combination of C–H activation and C–O ring-opening steps.

Complex **1** was also treated with neat thiophene. After the mixture was stirred at room temperature overnight, the color changed from green to red and the ¹H NMR spectrum displayed three new resonances in the aryl region (7.49, 7.39, and 7.24 ppm) in addition to the alkylidene hydrogen at 7.28 ppm. The ³¹P NMR spectrum also evinced two new doublets at 32.6 and 23.3 ppm (²J_{P–P} = 44 Hz), while the ¹³C{¹H} NMR spectrum further corroborated the formation of an alkylidene moiety with a resonance centered at 278.3 ppm. The four carbon resonances for thiophene were also present in the ¹³C{¹H} NMR spectrum, at 190.2, 149.1, 144.2, and 133.2 ppm. Although we were unable to obtain single crystals suitable for X-ray diffraction studies, the spectroscopic data are clearly consistent with formation of (PNP)Ti=CH¹Bu(*o*-C₄H₃S) (**15**) (Scheme 15). Complex **15** is reasonably stable at 60 °C, but at 100 °C it decomposes into a myriad of products, comprising mainly protonated ligand, (PNP)H. No ring-opened thiophene product was isolated or detected, as assayed by ¹H and ¹³C{¹H} NMR spectroscopy of the reaction mixture.

Addition of piperidine to **1** resulted in N–H activation and formation of a new species that we propose to be (PNP)Ti=CH¹Bu(NC₅H₁₀) (**16**) (Scheme 15) on the basis of multinuclear NMR spectroscopy. Complex **16** displayed two doublets in the ³¹P NMR spectrum (²J_{P–P} = 44 Hz), and the ¹H and ¹³C{¹H} NMR spectra further corroborated the

(68) Schmidbaur, H.; Stuehler, H.; Vornberger, W. *Chem. Ber.* **1972**, *105*, 1084.

Scheme 16. Proposed Sigmatropic Shift along the Denitrogenation Sequence



formation of a neopentylidene ligand in **16**. For instance, the alkylidene proton was located at 6.65 ppm in the ^1H NMR spectrum, whereas the alkylidene carbon was found at 278.4 ppm in the ^{13}C NMR spectrum. The resonances corresponding to the piperidine moiety could be located further upfield at 4.23 and 3.48 ppm, and we observed a broad resonance at 1.58 ppm. Complex **16** is thermally robust, but temperatures reaching or exceeding 100 °C resulted in a myriad of products, including (PNP)H. No evidence of β -hydride elimination and imine formation was observed.³⁶ Since activation of the N–H bond of piperidine can also result from σ -bond metathesis with the neopentyl ligand or 1,2-NH addition across the Ti=C ligand in **1**, both of which would not proceed through intermediate **A**, we conducted isotopic labeling studies using **1-d₃** and piperidine. The addition of piperidine to **1-d₃** followed by stirring for 12 h resulted in the formation of **16**, with no deuterium being incorporated into the alkylidene moiety when the mixture was examined by ^2H NMR spectroscopy, thereby suggesting that the transient alkylidyne intermediate **A** is most likely formed during this reaction. Our work complements previous studies by Legzdins and co-workers on 16e allene nitrosyl tungsten complexes that can also activate N–H bonds of pyrrolidine and piperidine.⁶⁹

Conclusions

Because HDN can be promoted or inhibited by the diverse substrates present in the oil feed stocks, detailed studies including the kinetics of this industrial process can only provide a few clues on how a specific substrate or a class of substrates can be activated. The composition and concentration of various N-heterocycles in different batches of crude oil can be dramatically different, so the interpretation of results can vary from one sample to another depending on the batch being used.²⁷ Despite these intrinsic limitations, many modifications of the Langmuir–Hinselwood model have been used to estimate the rate expression of this complex heterogeneous reaction in the past.²⁷ In the case of pyridine, extensive studies have concluded that the ring opening in piperidine, the hydrogenation product of pyridine, can be overall rate determining in the HDN once equilibrium is established²⁷ and that an increase in H_2 pressure has little influence on the rate for HDN of pyridine when a sulfide-modified NiMoP/Al₂O₃ catalyst is used at 300 °C.⁷⁰ Likewise, when metal nitrides were studied in the HDN of pyridine, it was observed that lower pressures of H_2

approaching 1 atm also had little to no effect on HDN and that such a decay of the N-heterocycle depended more heavily on the nature of the metal nitride than on the pressure of H_2 .⁷¹ Our current work determined that the concentration or nature of ClSiR₃ had very little effect on the N-removal process. Although our work is not directly correlated to the industrial HDN process, since no H_2 is being used in our study, we believe that these reactions might share some similarities, especially during the C–N bond cleavage process and possibly the N removal. In particular, the role of the Ti–alkylidyne moiety in promoting the pyridine ring opening is enlightening, because it demonstrates that metal–ligand multiple bonds can be active players during the C–N bond cleavage step. In this work, we concluded that ring opening of pyridine via the transient intermediate **A** is not rate determining in the C–N ring-opening process and also not overall rate determining in the N-removal process. The mechanism most consistent with our combined theoretical and experimental work involves hydrogen migration and a six- π -electrocyclic rearrangement being the most important steps along the denitrogenation reaction pathway. The interconversion of compounds **2–4** to the putative intermediate **D** might be best described as a sigmatropic rearrangement rather than a 1,3-hydrogen shift, therefore possibly invoking the alkylidene tethered carbene intermediate shown in Scheme 16. This scenario is a reasonable alternative, as the hybridization at the strained α -carbon atom accepting the H^+ must change in order to make the transfer possible. Our study demonstrated that the electrophile serves more as a trap rather than a promoter along the denitrogenation reaction, since slow pre-equilibrium steps might be dominating such a process. We speculate this to be true on the basis of our intuitive assertion that there is no significant energetic difference between **A** and the isoelectronic nitride (PNP)Ti \equiv N. However, this is presently speculative, since we have not conducted a detailed theoretical analysis of such a hypothetical nitride. Exploring a wider range of N-heterocycles and further computational studies (especially for (PNP)Ti \equiv N) should provide clues of which step is slow along the overall metathesis of N for C^tBu in substrates such as pyridine, and these avenues are currently being explored.

Acknowledgment. We thank Indiana University–Bloomington, the Dreyfus Foundation, the Sloan Foundation, and the NSF (No. CHE-0848248 to D.J.M. and No. CHE-0645381 to M.-H.B.) for financial support of this research. M.-H.B. is a Cottrell Scholar of Research Corp. A.R.F. acknowledges IU-Chemistry, the Bernice Eastwood Covalt Memorial, the James H. Coon Science Prize, and the College of Arts and Sciences for financial support. D.J.M. thanks Prof. S. E. Denmark for advice and insightful discussion.

Supporting Information Available: Text, figures, tables, and a CIF file giving synthetic details and complete characterization data for new complexes, kinetic studies, computational details, and Cartesian coordinates of all structures. This material is available free of charge via the Internet at <http://pubs.acs.org>.

(69) (a) Tsang, J. Y. K.; Fujita-Takayama, C.; Buschhaus, M. S. A.; Patrick, B. O.; Legzdins, P. *J. Am. Chem. Soc.* **2006**, *128*, 14762. (b) Tsang, J. Y. K.; Buschhaus, M. S. A.; Fujita-Takayama, C.; Patrick, B. O.; Legzdins, P. *Organometallics* **2008**, *27*, 1634.

(70) (a) Machida, M.; Sako, Y.; Ono, S. *Appl. Catal.* **2000**, *201*, 115. (b) Machida, M.; Sakao, Y.; Ono, S. *Appl. Catal.* **1999**, *187*, L73.

(71) Milad, I. K.; Smith, K. J.; Wong, P. C.; Mitchell, K. A. R. *Catal. Lett.* **1998**, *52*, 113.